

## Fluorene-based Tau Fibrillation Sensor and Inhibitor with Fluorogenic and Photo-crosslinking Properties.

Qiuxuan Xia<sup>‡a,b</sup>, Zhiming Wang<sup>‡a,c</sup>, Wang Wan<sup>a</sup>, Huan Feng<sup>a,b</sup>, Rui Sun<sup>a,b</sup>, Biao Jing<sup>a,c</sup>,  
Yusong Ge<sup>\*c</sup>, Yu Liu<sup>\*a</sup>

- a CAS Key Laboratory of Separation Science for Analytical Chemistry, Dalian Institute of Chemical Physics, Chinese Academy of Sciences, 457 Zhongshan Road, Dalian 116023, China.
- b University of Chinese Academy of Sciences, Beijing 100049, China.
- c The Second Hospital of Dalian Medical University, 467 Zhongshan Road, Dalian, 116023, China.

‡ These authors contributed equally.

\* Corresponding authors:

Yusong Ge – The Second Hospital of Dalian Medical University, 467 Zhongshan Road, Dalian 116023, China.; Email: [geyusongmed@sina.com](mailto:geyusongmed@sina.com)

Yu Liu – Dalian Institute of Chemical Physics, Chinese Academy of Sciences, 457 Zhongshan Road, Dalian 116023, China. <https://orcid.org/0000-0002-0779-1488>;  
Email: [liuyu@dicp.ac.cn](mailto:liuyu@dicp.ac.cn)

## Table of contents

<b>1. Experimental Methods</b>	<b>S3-S9</b>
1.1 Resistance to precipitation from H <sub>2</sub> O	
1.2 Fluorescence spectra measurement	
1.3 Viscosity dependence measurement and calculation	
1.4 Measurement of quantum yield	
1.5 Plasmids construction and protein purifications	
1.6 Monitoring tau protein aggregation kinetics	
1.7 Measurement of $K_d$ value between A4 and aggregated tau proteins	
1.8 Detection linear range and lowest limit of detection	
1.9 Chemical crosslinking to identify the presence of misfolded soluble oligomers	
1.10 Fluorescence intensity to demonstrate A4 could detect tau protein early misfolding state	
1.11 MTT assay	
1.12 Confocal imaging of aggregated tau proteins in stressed transfected HeLa cells	
1.13 General reactive oxygen species (ROS) detection	
1.14 ROS efficiency measurement	
1.15 ROS partition definition	
1.16 TEM images of tau proteins under light illumination and photosensitizer	
1.17 A4-OMe photo-crosslinked Tau to inhibit its aggregation	
1.18 Synthetic procedures	
<b>2. Supplementary Figures</b>	<b>S10-S23</b>
<b>3. Synthetic Procedures</b>	<b>S24-S27</b>
<b>4. NMR Spectra</b>	<b>S28-S37</b>
<b>5. References</b>	<b>S38-S39</b>

# 1. Experimental Methods

## 1.1 Resistance to precipitation from H<sub>2</sub>O

A3 and A4 (100 μM) were dissolved in deionized water (10 mL) and kept at 37 °C in water bath, respectively. At indicated time points, clear supernatant was pipetted into NEST 96 flat bottom transparent plates. The absorption spectra were collected at 404 nm for A3, 433 nm for A4 on Tecan Spark Fluorescence Plate Reader. Error bar: standard error (n = 3).

## 1.2 Fluorescence spectra measurement

A series and B series probes from a 1 mM DMSO stock solution was diluted to 50 μM. 100 μL of each sample was pipetted into a BeyoGold™ 96-Well Black Opaque plate to measure the fluorescence intensity. Fluorescence spectra were collected using a Tecan Spark Fluorescence Plate Reader. Each spectrum was normalized against its maximal fluorescence intensity.

## 1.3 Viscosity dependence measurement and calculation (Fig 2b, 2c)

To minimize the impact of solvent polarity on the fluorescence emission intensity, glycerol-ethylene glycol mixture was chosen for the measurement of viscosity sensitivity due to their similar polarity (dielectric constants of glycerol = 46.5, dielectric constants of ethylene glycol = 37.0).

Solutions of different viscosity were prepared by changing the percentage of glycerol in ethylene glycol as 0%, 20%, 40%, 60%, 80%, and 100% (volume fraction). Viscosity of the mixtures was calculated according to the previously reported method.<sup>[1]</sup> The mixture viscosity ( $\eta_{\text{mix}}$ ) can be calculated using Eq. S1 (viscosity of glycerol = 1500.00 mPa·s, viscosity of ethylene glycol = 25.66 mPa·s).

$$\ln \eta_{\text{mix}} = \sum_{i=1}^n w_i \cdot \ln \eta_{\text{mix}} \quad (\text{S1})$$

glycerol in glycol (volume %)	viscosity (mPa·s)
0	25.66
20	62.98
40	147.75
60	332.34
80	718.95
100	1500.00

All tested sample solutions were diluted from 1 mM DMSO stock solution to 20 μM. Fluorescence emission spectra were collected using a Tecan Spark Fluorescence Plate Reader in BeyoGold™ 96-Well Black Opaque plates. Excitation wavelength was 456 nm for A4.

The viscosity-dependent curve was plotted using logarithm of solvent viscosity as X-

axis and logarithm of emission intensity as Y-axis, and the viscosity dependence parameter  $x$  was determined based on the Förster-Hoffmann equation (Eq. S2).

$$\log I = x \log \eta + C \quad (\text{S2})$$

In which  $I$  is the fluorescence intensity,  $\eta$  is viscosity,  $x$  is the viscosity sensitivity,  $C$  is a constant and  $x$  represents the sensitivity of the fluorescent probe to the viscosity. Error bar: standard error ( $n = 3$ ).

#### 1.4 Measurement of quantum yield

Quantum yield was measured according to a published guideline.<sup>[2]</sup> Nile blue ( $\phi = 0.27$ , ethanol) was selected as the standard material. Nile blue was diluted with ethanol to 10, 8, 4, 2  $\mu\text{M}$  to measure absorbance and emission intensity. UV-vis absorption spectra and fluorescence spectra were collected on Tecan Spark Fluorescence Plate Reader using Costar™ 96-Well Transparent plates with ultra-low attachment surface for fluorescence measurements, respectively. Based on the spectra of Nile Blue probes, 456 nm was selected as the excitation wavelength for A4 (in aggregated Tau). The quantum yield was calculated based on the equation (Eq. S3).

$$\phi = \phi_{\text{ST}} \cdot (\text{Grad}_x / \text{Grad}_{\text{ST}}) \cdot (\eta_x / \eta_{\text{ST}})^2 \quad (\text{S3})$$

Where the  $\phi$  is the quantum yield,  $\eta$  is the refractive index of solvent at 25 °C and subscripts  $x$  and ST stand for probes-of-interest and standard material, respectively. For the testing sample, slope of absorbance to concentration is  $k_1$ , the slope of integrated fluorescence emission to concentration is  $k_2$ , and  $\text{Grad}_x = k_2/k_1$ ; for the standard sample, gradient of absorbance to concentration is  $k_3$ , the gradient of integrated fluorescence emission to concentration is  $k_4$ , and  $\text{Grad}_{\text{ST}} = k_4/k_3$ . Error bar: standard error ( $n = 3$ ).

#### 1.5 Plasmids construction and protein purifications

Genes of TauK18 wild type (TauK18-WT) and TauK18-P301L-mCherry were first codon optimized, synthesized by GenScript, Nanjing, China, and sub-cloned into pET-29b(+) vectors and pcDNA3.1(+) vectors respectively. For easy purification, these proteins were cloned with His-tag and TEV cleavage site at the C-termini.

TauK18-WT protein plasmid was transformed into BL21(DE3) *E. coli* cells. Cells were grown to  $\text{OD}_{600}$  in the range of 0.6-0.8 before induced by IPTG (0.4 mM), then the temperature was decreased to 16 °C and the culture was allowed to grow overnight. The following day, cells were harvested by centrifugation and resuspended in lysis buffer [50 mM Tris, 500 mM NaCl, and 10 mM imidazole (pH = 8.00) at 4 °C]. Cells expressing recombinant proteins were thawed and lysed by sonication at 4 °C. Lysed cells were centrifuged at 30700 g for 30 min. The supernatant was collected and loaded onto a 10 mL Ni-NTA column and washed with buffer [50 mM Tris, 500 mM NaCl, and 500 mM imidazole (pH = 8.00) at 4 °C]. The eluent was buffer exchanged back into 10  $\mu\text{M}$  imidazole buffer during an incubation with 1 mM DTT and 1~2 ml 5U/ $\mu\text{L}$  TEV protease overnight at 4 °C. This solution was then run over the Ni-NTA column, and the flow-through was

collected and concentrated to 1–2 mL using a 3 kDa molecular weight cutoff centrifugal filter. The protein fractions were identified by SDS-PAGE analysis, pooled, and concentrated. Further purification of proteins was carried on 120 mL Superdex 200 size-exclusion column in phosphate buffer [10 mM sodium phosphates, 100 mM KCl, 1 mM EDTA, acidified by HCl (pH = 7.40)]. Fractions containing target proteins were identified by SDS-PAGE gel analysis, pooled, and concentrated. The purity was estimated > 95% with on significant impurities based on SDS-PAGE gel.<sup>[3]</sup>

### 1.6 Monitoring tau protein aggregation kinetics (Fig 1, Fig 2e)

Freshly purified tau protein (25  $\mu$ M) and probe (10  $\mu$ M) were mixed in aggregation buffer [phosphate buffer (10 mM sodium phosphate, 100 mM KCl, 1 mM EDTA, pH = 7.40), heparin 2.5  $\mu$ M, DTT 1 mM] and stored at 37 °C. A volume of 100  $\mu$ L of the mixture was pipetted into a Costar™ 96-Well Transparent plates with ultra-low attachment surface to measure the fluorescence intensity at indicated time. The fluorescence emission spectra were collected using the Tecan Spark Fluorescence Plate Reader. ThT was selected as a positive control under the identical experimental condition. Each spectrum was normalized against ThT maximal fluorescence intensity (A1:  $\lambda_{ex}$  = 408 nm,  $\lambda_{em}$  = 472 nm; A2:  $\lambda_{ex}$  = 435 nm,  $\lambda_{em}$  = 545 nm; A3:  $\lambda_{ex}$  = 466 nm,  $\lambda_{em}$  = 707 nm; A4:  $\lambda_{ex}$  = 456 nm,  $\lambda_{em}$  = 684 nm; B1:  $\lambda_{ex}$  = 490 nm,  $\lambda_{em}$  = 674 nm; B2:  $\lambda_{ex}$  = 512 nm,  $\lambda_{em}$  = 607 nm; B3:  $\lambda_{ex}$  = 430 nm,  $\lambda_{em}$  = 663 nm; ThT:  $\lambda_{ex}$  = 440 nm,  $\lambda_{em}$  = 480 nm). Error bars: standard error (n = 3).

**Note:** If not specifically stated, the subjects (centrifuge tubes, tips, and 96-well plates, etc) used for *in vitro* tau protein experiments are ultra-low adsorption materials.

### 1.7 Measurement of $K_d$ value between A4 and aggregated tau proteins (Fig 2d)

Solutions of tau protein (25  $\mu$ M) and probe A4 of gradient concentrations (from 0.005 to 50  $\mu$ M) in aggregation buffer [phosphate buffer (10 mM sodium phosphate, 100 mM KCl, 1 mM EDTA, pH = 7.40), heparin 2.5  $\mu$ M, DTT 1 mM] were incubated at 37 °C for 24 h to induce tau protein aggregation. Then, the fluorescence of aggregated protein-A4 binding complex was measured by a Tecan Spark Fluorescence Plate Reader. Error bars: standard error (n = 3).

The dissociation constant ( $K_d$ ) of the aggregated protein-probe interaction was then obtained by nonlinear regression fitting based on the equation (Eq. S4), using GraphPad Prism 6.0.

$$Y = \frac{X * B_{max}}{Kd + X} \quad (S4)$$

Where Y was the fluorescence of probe binding to aggregated tau proteins and  $B_{max}$  represented the maximal fluorescence, X was the concentration of probe.

### 1.8 Detection linear range and lowest limit of detection (Fig 2d)

The experiment followed the **Experimental Methods 1.7**. The concentration-dependent fluorescence intensity of A4 showed linearity between 50 nM - 2  $\mu$ M. The lowest limit of detection was down to 50 nM, with a fold-of-change (FOC) = 2.98. Error bars: standard error (n = 3).

### **1.9 Chemical crosslinking to identify the presence of misfolded soluble oligomers (Fig 2f)**

SDS-PAGE gel of chemically crosslinked DHFR soluble oligomers was visualized by Coomassie brilliant blue staining. Freshly purified tau protein (100  $\mu$ M) was dissolved in aggregation buffer [phosphate buffer (10 mM sodium phosphate, 100 mM KCl, 1 mM EDTA, pH = 7.40), heparin 2.5  $\mu$ M, DTT 1 mM] and stored at 37 °C. At indicated time, 100  $\mu$ L of prepared samples were treated with 5  $\mu$ L 30 mM DSS (disuccinimidyl suberate) at 25 °C for 10 min, and then quenched the crosslinking reaction by adding 2  $\mu$ L 1 M Tris-HCl buffer (pH = 7.40). The well mixed samples were incubated at 25 °C for 10 min followed by incubating with 25  $\mu$ L 5X loading buffer (2.0% sodium dodecyl sulfate, 0.1% Bromophenol blue) at 95 °C for 5 min. The samples were loaded on to a 12% acrylamide SDS-PAGE gel for electrophoresis analysis. To visualize the presence of crosslinked soluble oligomers, the gel was stained with Coomassie brilliant blue. BeyoTime™ Protein Marker served as the protein molecular weight ladder on SDS-PAGE gel.

### **1.10 Fluorescence intensity to demonstrate A4 could detect tau protein early misfolding state (Fig 2f)**

The experiment followed the **Experimental Methods 1.9**. Freshly purified tau protein (25  $\mu$ M) and ThT (10  $\mu$ M) or A4 (10  $\mu$ M) were dissolved in aggregation buffer [phosphate buffer (10 mM sodium phosphate, 100 mM KCl, 1 mM EDTA, pH = 7.40), heparin 2.5  $\mu$ M, DTT 1 mM] and stored at 37 °C, respectively. At indicated time, 100  $\mu$ L of prepared samples were pipetted into a Costar™ 96-Well Transparent plates with ultra-low attachment surface to measure the fluorescence intensity. The fluorescence emission spectra were collected using the Tecan Spark Fluorescence Plate Reader. Each spectrum was normalized against A4 maximal fluorescence intensity (A4:  $\lambda_{ex}$  = 456 nm,  $\lambda_{em}$  = 684 nm; ThT:  $\lambda_{ex}$  = 440 nm,  $\lambda_{em}$  = 480 nm). Error bars: standard error (n = 3).

### **1.11 MTT assay**

The effect of probe A4 and A4-OMe on the viability of cells was detected by MTT assay. The HeLa cells (1X10<sup>4</sup>/well in 200  $\mu$ L medium) were seeded into 96-well plate and incubated for 24 h. After treatment with probe (0, 0.5, 1, 2, 5  $\mu$ M) for 24 h, the viability of the cancer cells was detected with MTT. 20  $\mu$ L of MTT solution (5 mg/ml in PBS) was added to each well, and the mixtures were incubated for 4 h at 37 °C, 5% CO<sub>2</sub>. Then, removed the medium containing MTT and added 150  $\mu$ L DMSO to each well, shook for 10 min to make the crystal dissolve completely. The OD<sub>570</sub> of each sample was measured on Spark Fluorescence Plate Reader. Error bars: standard error (n = 3).

### **1.12 Confocal imaging of aggregated tau proteins in stressed transfected HeLa cells (Fig 3d)**

HeLa cells were seeded on 35 mm confocal culture dishes and transiently transfected when the cell density reached 70%. In 50  $\mu$ L opti-mem medium, 1.25  $\mu$ L of lip3000 was added and incubated at room temperature for 5 min (mixture a). In another 50  $\mu$ L opti-mem medium, 8  $\mu$ L of P3000 and plasmid DNA of TauK18-P301L-mCherry (4  $\mu$ g for each transfection) were added and incubated at room temperature for 5 min (mixture b). The

above mixture a and mixture b were mixed and incubated at room temperature for 20 min to obtain mixture c. The mixture c and probe (0.5  $\mu\text{M}$  A4 or A4-OMe) were then dripped into the cell medium and allowed expressing for 24 h. Okadaic acid (10 nM) was introduced into the media and incubated for another 24 h. Hoechst 33342 staining reagent was added into cell medium and incubated for 30 minutes before imaging. Confocal fluorescence images were collected by using Olympus FV1000MPE. Blue: 405 nm for Hoechst 33342; Green: 488 nm for A4 and A4-OMe; Red: 543 nm for TauK18-P301L-mCherry.

### 1.13 General reactive oxygen species (ROS) detection (Fig 4b)

General ROS yielded by probes under white light illumination was detected by 2,7-dichlorodihydrofluorescein (DCFH) with fluorescence analysis.<sup>[4]</sup> DCFH, herein, was converted from dichlorofluorescein diacetate (DCF-DA). Specifically, DCF-DA (1 mM in ethanol, 0.5 mL) was hydrolyzed by NaOH (10 mM, 2 mL) for 30 min at room temperature. The obtained hydrolysate was then neutralized by 10 mL PBS to get DCFH stock solution (40  $\mu\text{M}$ ), which was further stored at  $-20\text{ }^{\circ}\text{C}$  in dark. During the detection process, 10  $\mu\text{M}$  DCFH was used to mix with A4-OMe (3  $\mu\text{M}$ ) and the fluorescence changes of DCFH at 525 nm were collected ( $\lambda_{\text{ex}} = 488\text{ nm}$ ) at different light irradiation time. The fluorescence emission spectra were collected using the Tecan Spark Fluorescence Plate Reader. Rose Bengal was selected as a positive control under the identical experimental condition. Error bars: standard error (n = 3).

### 1.14 ROS efficiency measurement

According to previous reports in the literature,<sup>[5]</sup> the ROS quantum yield was determined based on the following simple equation:

$$\Phi_{\text{ROS}} = \frac{K_{\text{probe}}}{A_{\text{probe}}} \quad (\text{S5})$$

Where  $K_{\text{probe}}$  was the oxidation rate constant of DCFH by the ROS produced by probes versus irradiation time,  $A_{\text{probe}}$  was the absorption ability of probes.  $\Phi_{\text{ROS}}(\text{A4-OMe}) = 2.30$ ,  $\Phi_{\text{ROS}}(\text{Rose Bengal}) = 1.92$ . Error bars: standard error (n = 3).

### 1.15 ROS partition definition (Fig 4c)

*Singlet oxygen ( $^1\text{O}_2$ ) detection.*

$^1\text{O}_2$  measurement was conducted using 9,10-Anthracenediyl-bis(methylene) (ABDA) as the selective indicator.<sup>[6]</sup> 10 mM stock solution ABDA was prepared in DMF and stored in light-free conditions at  $-20\text{ }^{\circ}\text{C}$ . In practice use, the ABDA stock solution was diluted into 0.1 mM and mixed with probes (3  $\mu\text{M}$ ). In this experiment, the absorbance decline of ABDA reacted with singlet oxygen at 378 nm was recorded at different light irradiation time. The absorbance spectra were collected using the Tecan Spark Fluorescence Plate Reader. Rose Bengal was selected as a positive control under the identical experimental condition. Error bars: standard error (n = 3).

*Superoxide anion radical ( $\text{O}_2^{\cdot -}$ ) detection.*

Dihydrorhodamine 123 (DHR 123), which can be specifically reacted with  $\text{O}_2^{\cdot -}$  among ROS species, was used as the superoxide anion radical detector.<sup>[6]</sup> Stock solution (10 mM) of DHR 123 was prepared in DMF and stored at  $-20\text{ }^{\circ}\text{C}$  with light-free. In practice use,

diluted DHR 123 (6  $\mu\text{M}$ ) was used to detect the  $\text{O}_2^{\cdot-}$  produced by probes (3  $\mu\text{M}$ ) and fluorescence intensity at 525 nm was recorded ( $\lambda_{\text{ex}} = 480 \text{ nm}$ ) at different light irradiation time. The fluorescence emission spectra were collected using the Tecan Spark Fluorescence Plate Reader. Rose Bengal was selected as a positive control under the identical experimental condition. Error bars: standard error ( $n = 3$ ).

#### *Hydroxyl radical ( $\cdot\text{OH}$ ) detection.*

For  $\cdot\text{OH}$  detection, a commercially available kit, hydroxyphenyl fluorescein (HPF) was utilized.<sup>[7]</sup> Stock solution (1 mg/ml, 2.36 mM) of HPF was prepared in DMF and stored at  $-20^\circ\text{C}$  with light-free. In real test, diluted HPF (6  $\mu\text{M}$ ) was used to detect the  $\cdot\text{OH}$  produced by probes (3  $\mu\text{M}$ ) and fluorescence intensity at 514 nm was recorded ( $\lambda_{\text{ex}} = 480 \text{ nm}$ ) at different light irradiation time. The fluorescence emission spectra were collected using the Tecan Spark Fluorescence Plate Reader. Rose Bengal was selected as a positive control under the identical experimental condition. Error bars: standard error ( $n = 3$ ).

### **1.16 TEM images of tau proteins under light illumination and photosensitizer**

The illuminated sample was spotted on the carbon coated formvar grid (Beijing Zhongjingkeyi Technology Co.,Ltd., China) and incubated for 1 min. Then the grid was stained with 1% (w/w) phosphotungstic acid aqueous solution and baked with digital display infrared baking lamp (Elitech, TPM-910+, China) before imaging. The grids were subjected to transmission electron microscopy (TEM) imaging (JEM-2100, JEOL, Japan) at 200 kV. Images were recorded using Digital Microscopes Soft imaging.

### **1.17 A4-OMe photo-crosslinked Tau to inhibit its aggregation (Fig 4e, 4f)**

The experiment followed the **Experimental Methods 1.6**. Freshly purified tau protein (25  $\mu\text{M}$ ) and A4-OMe (10  $\mu\text{M}$ ) were mixed in aggregation buffer [phosphate buffer (10 mM sodium phosphate, 100 mM KCl, 1 mM EDTA, pH = 7.40), heparin 2.5  $\mu\text{M}$ , DTT 1 mM] and then illuminated under white light (25  $\text{mW}\cdot\text{cm}^{-2}$ ) for 1 h. ThT (10  $\mu\text{M}$ ) was introduced to the mixture after light illumination. To monitor tau protein aggregation kinetics, 100  $\mu\text{L}$  of the mixture was pipetted into a Costar™ 96-Well Transparent plates with ultra-low attachment surface to measure the fluorescence intensity at indicated time. The fluorescence emission spectra were collected using the Tecan Spark Fluorescence Plate Reader. Each spectrum was normalized against ThT maximal fluorescence intensity (ThT:  $\lambda_{\text{ex}} = 440 \text{ nm}$ ,  $\lambda_{\text{em}} = 480 \text{ nm}$ ). DMSO and Crystal Violet were selected as negative and positive control under the identical experimental condition, respectively. Error bars: standard error ( $n = 3$ ).

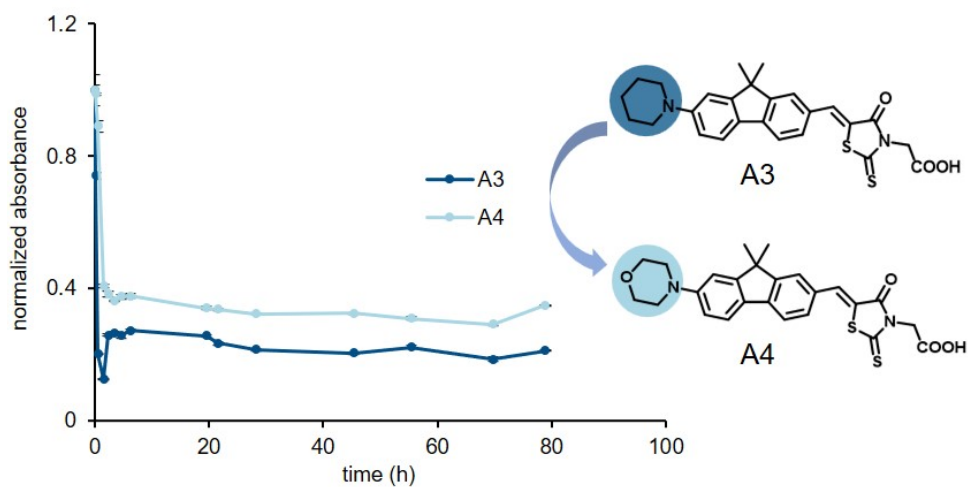
HEPES-TRIS gel of photo-crosslinked tau proteins was visualized by Coomassie brilliant blue staining. 100  $\mu\text{L}$  of the kinetic endpoint sample should be incubated with 25  $\mu\text{L}$  of 5X loading buffer (2.0% sodium dodecyl sulfate, 0.1% Bromophenol blue) at  $95^\circ\text{C}$  for 5 min. The well mixed samples were loaded on to a 4-20% HEPES-TRIS gel for electrophoresis analysis. To visualize the presence of crosslinked proteins, the gel was stained with Coomassie brilliant blue. BeyoTime™ Protein Marker served as the protein molecular weight ladder on HEPES-TRIS gel. Error bars: standard error ( $n = 3$ ).

### **1.18 Synthetic procedures**

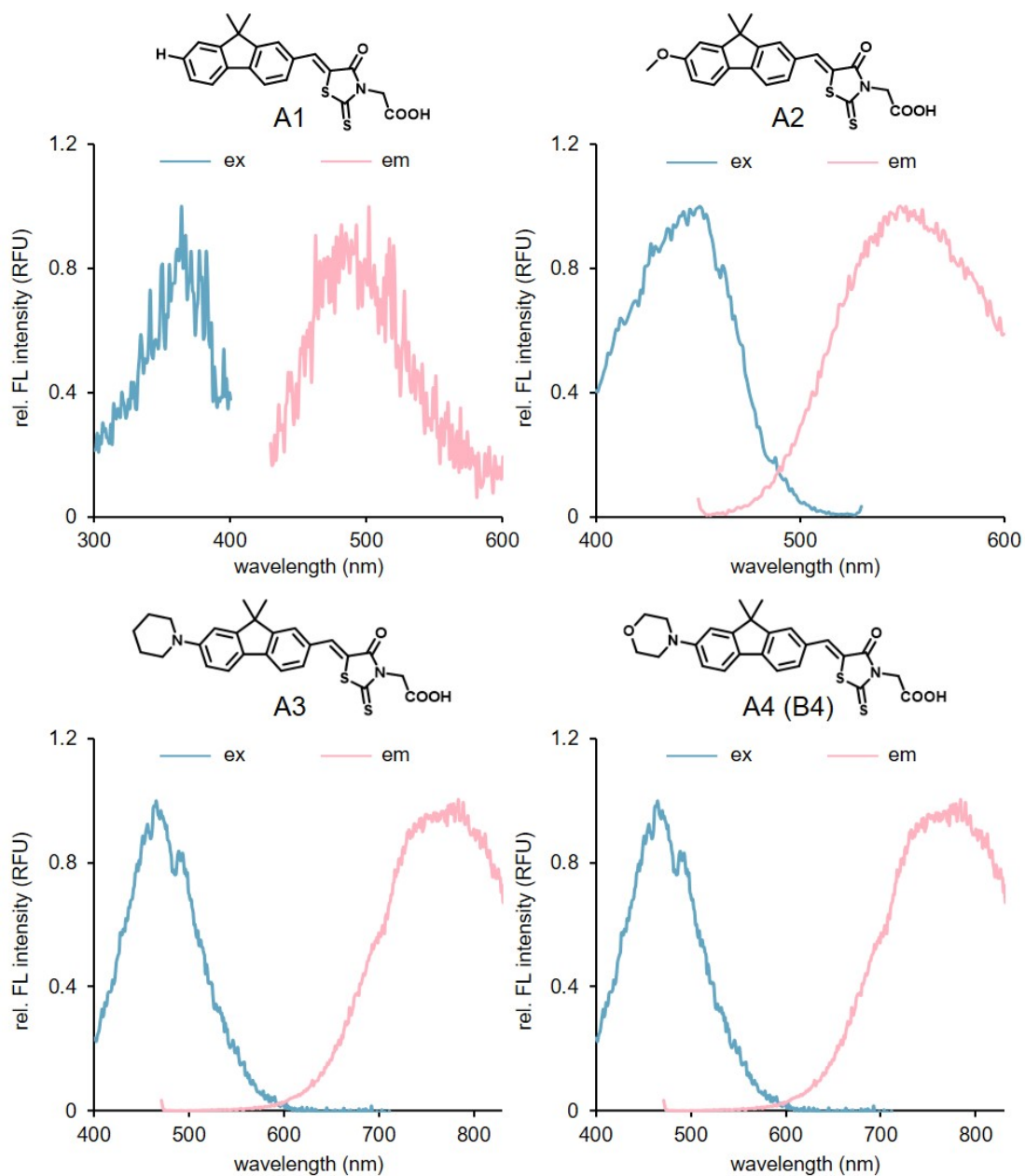


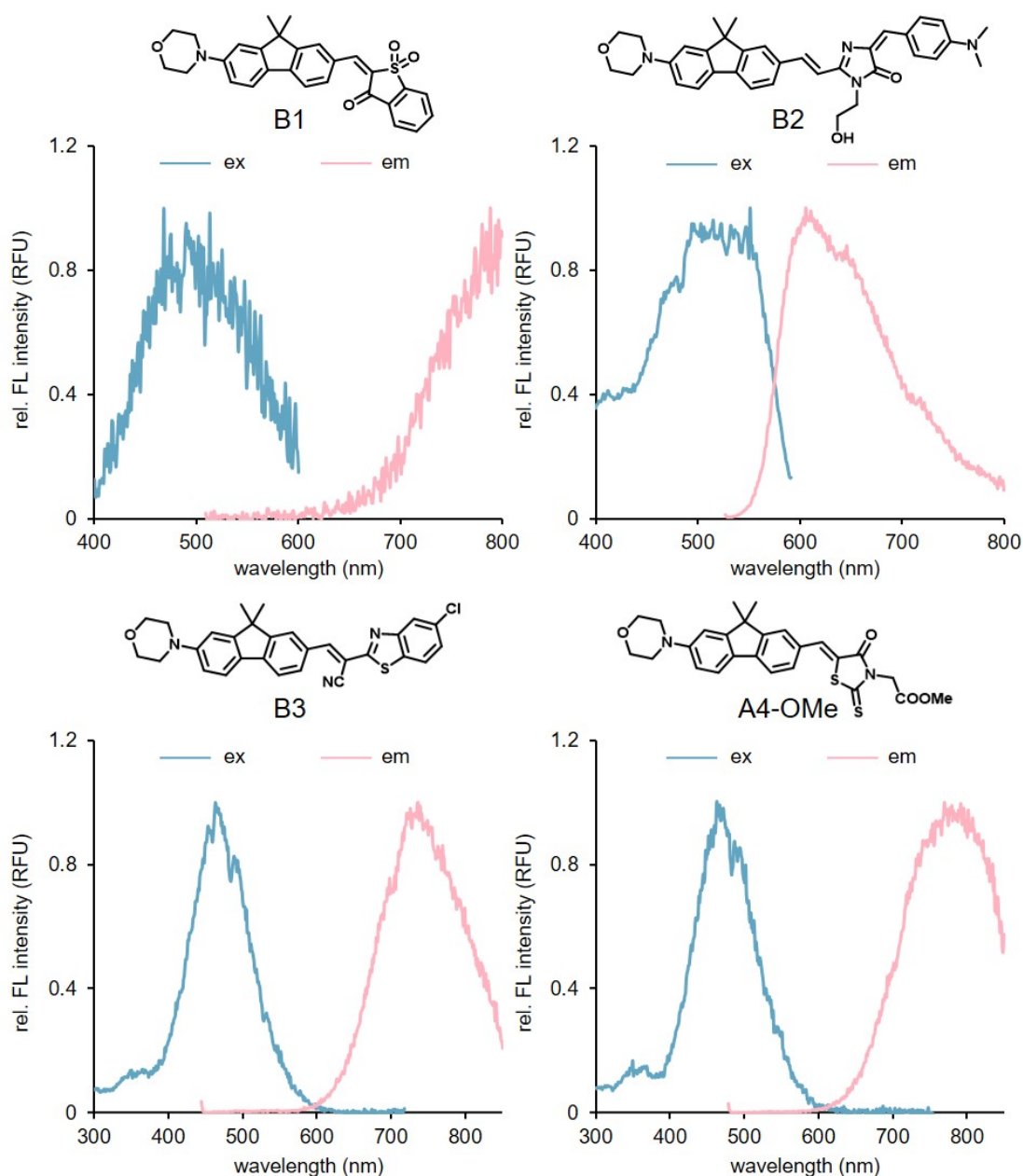
All reagents are commercial grade unless otherwise stated. Reactions were carried out in Synthware® round bottom flask and monitored via thin layer chromatograph. Products were purified with flash column chromatograph (200-300 mesh). NMR spectra were recorded on Bruker 400 MHz and 700 MHz spectrometers and were calibrated using residual solvent as an internal reference (CDCl<sub>3</sub>: 7.26 ppm for <sup>1</sup>H NMR and 77.16 ppm for <sup>13</sup>C NMR, DMSO-*d*<sub>6</sub>: 2.50 ppm for <sup>1</sup>H NMR and 39.52 ppm for <sup>13</sup>C NMR). HRMS data was obtained with Agilent 6540 Accurate-MS spectrometer (Q-TOF).

## 2. Supplementary Figures

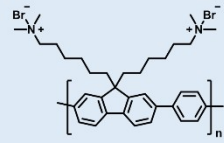
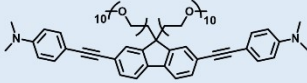
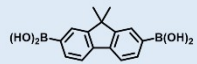
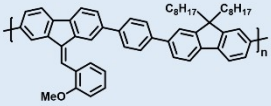
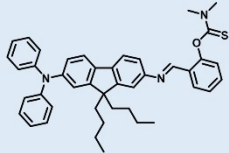
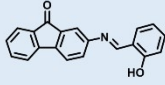
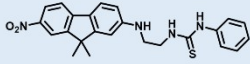


**Figure S1.** Morpholine group improves the solubility of the probe. A3 and A4 (100  $\mu$ M) were dissolved in deionized water (10 mL) and kept at 37  $^{\circ}$ C in water bath, respectively. At indicated time points, clear supernatant was pipetted into NEST 96 flat bottom transparent plates. The absorption spectra were collected at 404 nm for A3, 433 nm for A4 on Tecan Spark Fluorescence Plate Reader. A4 was more resistant towards precipitation from water measured by residual absorbance over 80 h incubation.

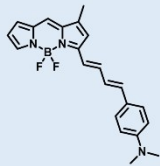
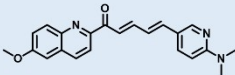
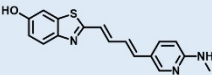
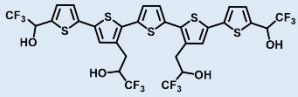
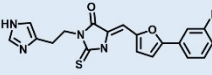
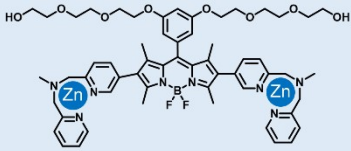




**Figure S2.** Normalized fluorescence excitation and emission spectra of probes in DMSO. Probes were prepared to 50  $\mu\text{M}$  for excitation scan and emission measurement. All measurements were carried out using Tecan Spark Fluorescence Plate Reader in NEST 96-Well flat bottom transparent plates. The experimental procedure followed **Experimental Methods 1.2**. All measurements were repeated for three times.

Structure	Targets	Reference
	DNA	Ref 8, 9
	Lysosome	Ref 10
	monosaccharide	Ref 11
	TNP	Ref 12
	Cu <sup>2+</sup>	Ref 13
	I <sup>-</sup>	Ref 14
	Hg <sup>2+</sup> , CH <sub>3</sub> Hg <sup>+</sup>	Ref 15

**Figure S3.** Summary of fluorene-based sensors in detection of biological species and bioimaging.

Structure	$K_d$	Reference
	/	Ref 16
	16.6 nM	Ref 17
	/	Ref 18
	66 nM	Ref 19
	$64 \pm 7$ nM	Ref 20
	7.5 $\mu$ M	Ref 21

**Figure S4.** Summary of different scaffolds to target tau protein. The slash represented that specific data was not provided in the original references.

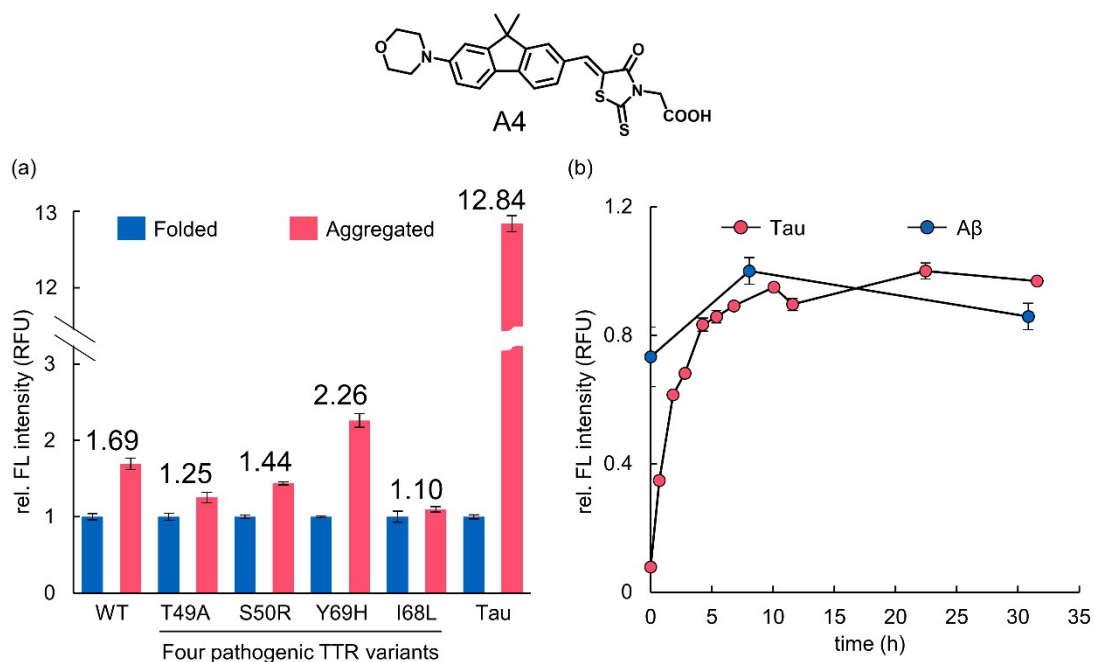


**Figure S5.** A4 selectively bind to aggregated Tau proteins. To evaluate the probe's selectivity, we utilized the pathogenic proteins transthyretin (TTR) and A $\beta$ , which are associated with cardiac amyloidosis and Alzheimer's disease, respectively. We did not observe substantial fluorescence changes in TTR or A $\beta$  compared to Tau protein. However, in case of tau protein, there was a significant 12.84-fold increase in fluorescence intensity. This experiment demonstrated the selectivity of A4 for tau protein over other amyloid proteins such as TTR and A $\beta$ . (a) Fluorescence change histograms showed different binding affinity between A4 and TTR (WT and four pathogenic variants) or tau proteins. (b) A4 monitored the fibrillation of tau but not A $\beta$  aggregation. Error bars: standard error (n = 3).

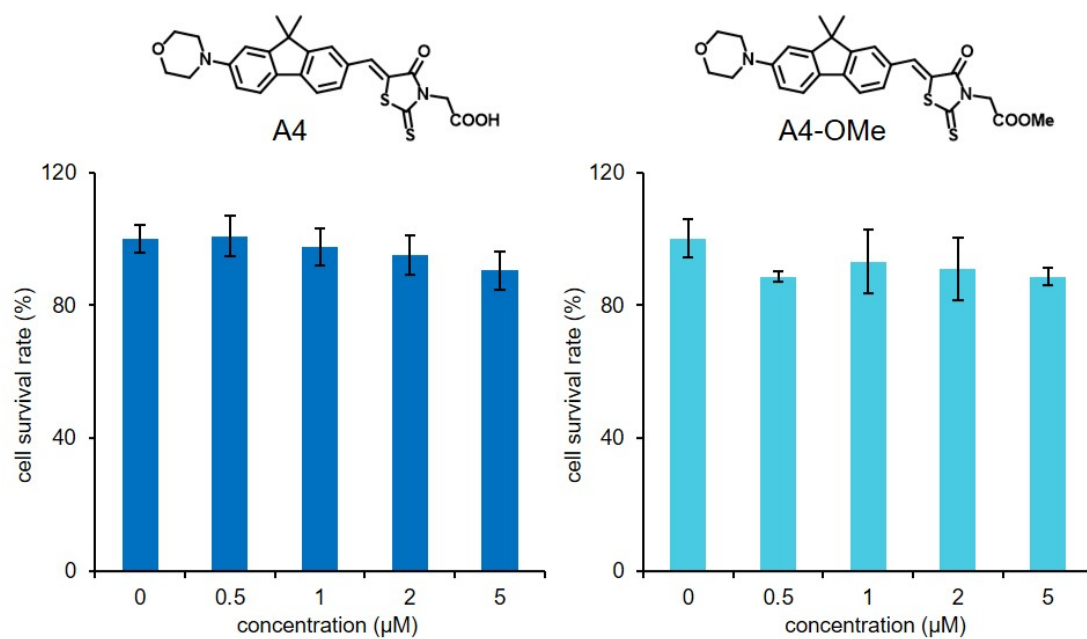


**Figure S6.** A4 and A4-OMe showed satisfactory cytotoxicity performance at working concentrations. In all imaging experiments, A4 and A4-OMe were used at the concentration less than 0.5  $\mu\text{M}$ . Cell viability was measured using MTT assay in HeLa cells. Error bars: standard error ( $n = 3$ ).



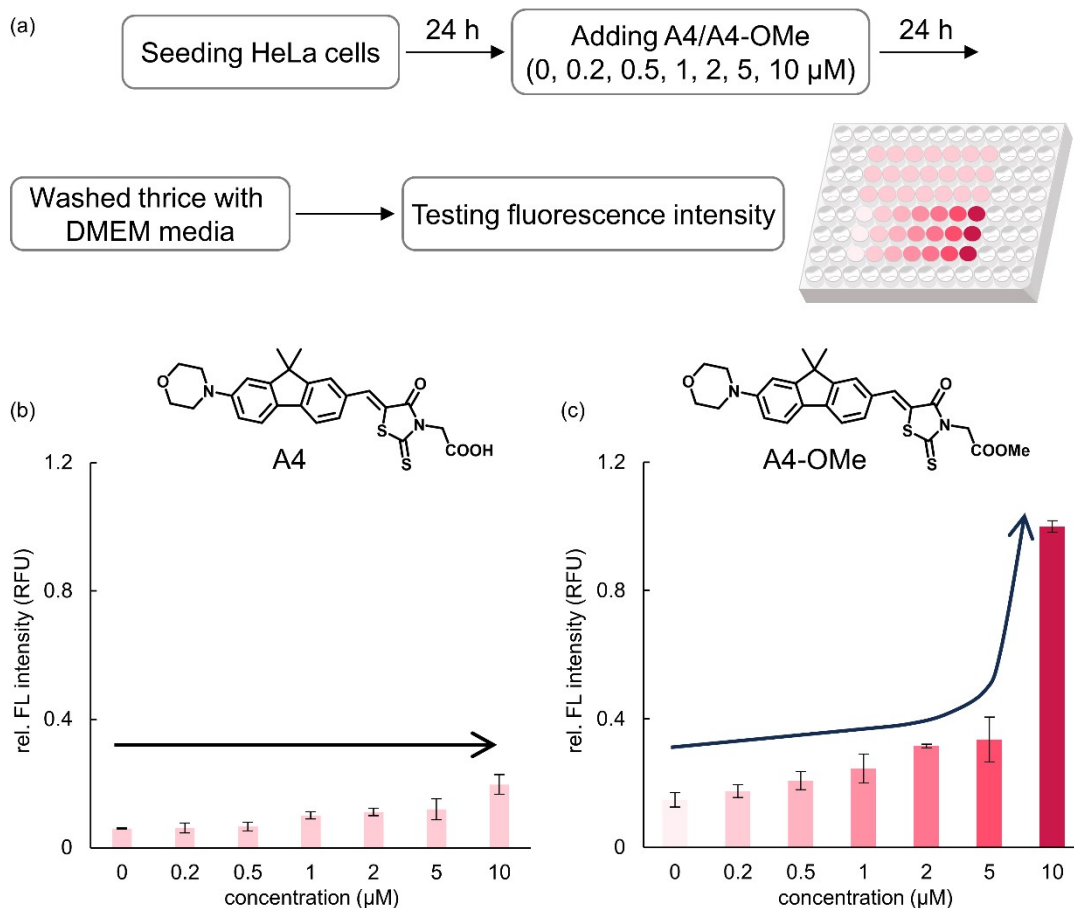


**Figure S7.** Cellular uptake test confirmed A4-OMe can effectively penetrate into the cells. The HeLa cells ( $1 \times 10^4$ /well in 200  $\mu\text{L}$  medium) were seeded into 96-well plate and incubated for 24 h. After treatment with probe A4/A4-OMe (0.0, 0.2, 0.5, 1.0, 2.0, 5.0, 10.0  $\mu\text{M}$ ) for 24 h, the cells were washed with DMEM media for three times. The fluorescence intensity of each sample was measured on Spark Fluorescence Plate Reader. Error bars: standard error ( $n = 3$ ). (a) Schematic diagram of the cellular uptake test of A4/A4-OMe. The fluorescence intensity response of (b) A4 and (c) A4-OMe to different probe's concentration in HeLa cells.

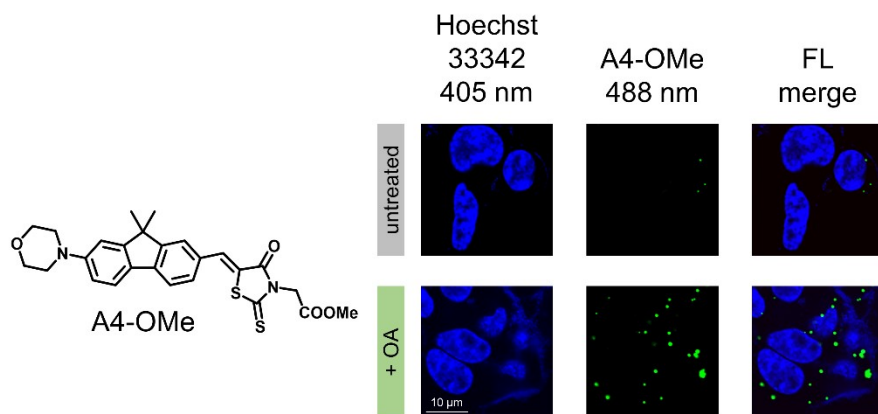


**Figure S8.** A4-OMe detected aggregated tau proteins in stressed SH-SY5Y cells. Fluorescence images of SH-SY5Y cells incubated with A4-OMe. Top: vehicle control, bottom: stressed with okadaic acid (10 nM) for 24 h. Scale bar: 10 µm.

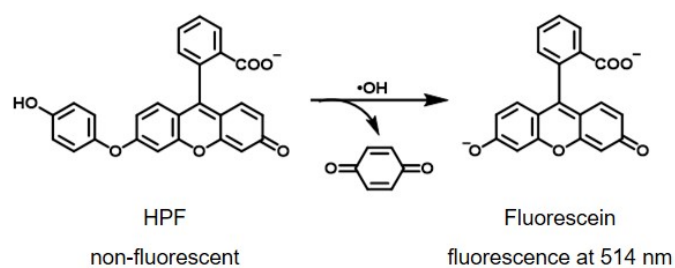
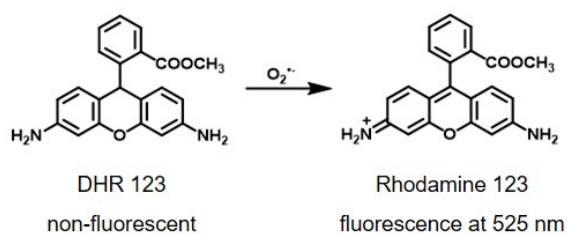
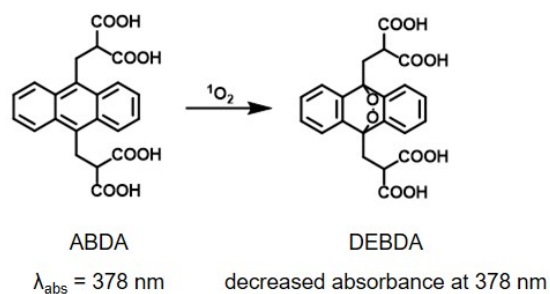
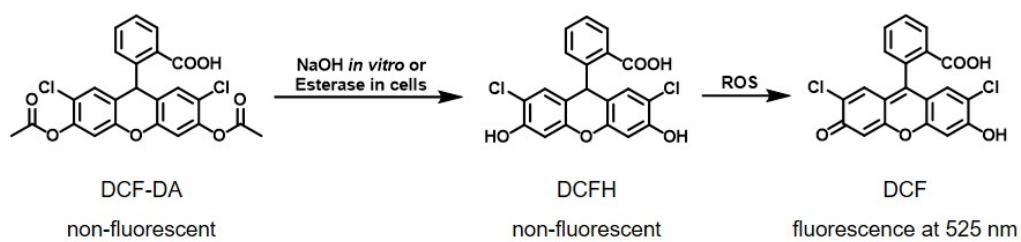


**Figure S9.** Sensing mechanism of DCFH, ABDA, DHR 123 and HPF in detecting general ROS, singlet oxygen, superoxide anions, and hydroxyl radicals, respectively.

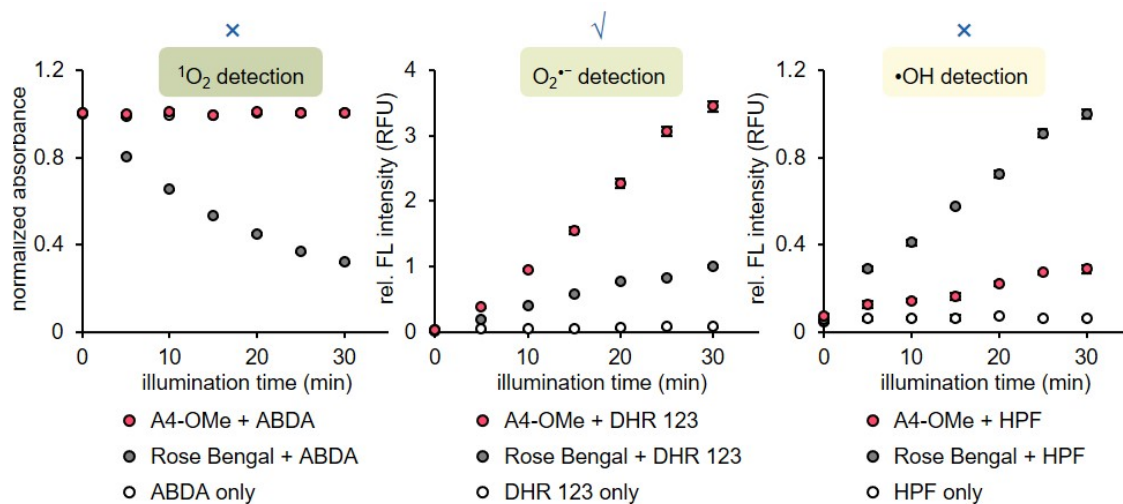


**Figure S10.** A4-OMe mainly generated superoxide anion and generated virtually no singlet oxygen and hydroxyl radicals, indicating that it underwent type-I photosensitization pathway.

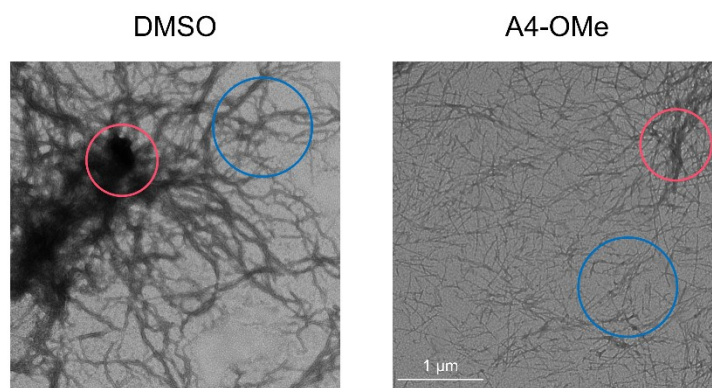


**Figure S11.** TEM images of tau proteins under light illumination and photosensitizer. First, freshly purified tau protein (25  $\mu\text{M}$ ) and DMSO or A4-OMe (10  $\mu\text{M}$ ) were mixed in aggregation buffer (phosphate buffer (10 mM sodium phosphate, 100 mM KCl, 1 mM EDTA, pH = 7.40), heparin 2.5  $\mu\text{M}$ , DTT 1 mM) and then illuminated under white light (25  $\text{mW}\cdot\text{cm}^{-2}$ ) for 1 h. The sample was then incubated at 37  $^{\circ}\text{C}$  for 24 h before being prepared for TEM imaging. Red circle: tau seeds, blue circle: tau fibrils. The TEM experimental procedure followed **Experimental Methods 1.16**. At least five different images from different regions of each grid were obtained for each sample and all showed similar conclusion. The illuminated product showed more Tau tangles and fibrillations.

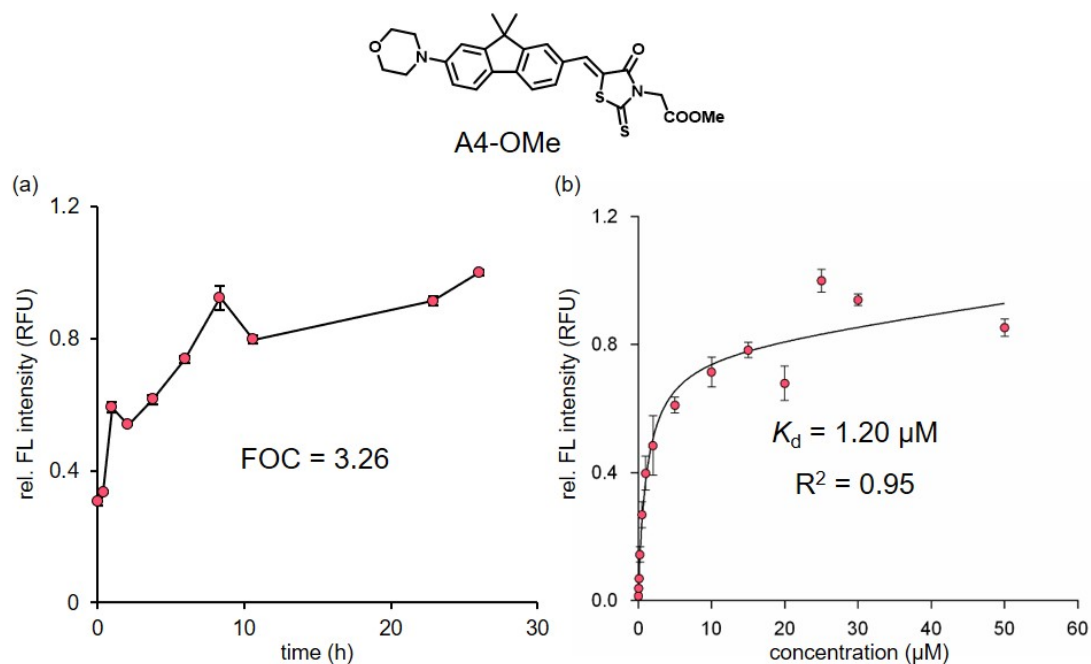


**Figure S12.** A4-OMe retained singlet fluorogenicity upon binding to aggregated tau proteins. (a) A4-OMe exhibited 3.26 fold-of-change upon binding to aggregated tau proteins. The experiment followed the **Experimental Methods 1.6**. (b) A4-OMe showed strong binding affinity to aggregated tau proteins ( $K_d = 1.20 \mu\text{M}$ ). The experiment followed the **Experimental Methods 1.7**.

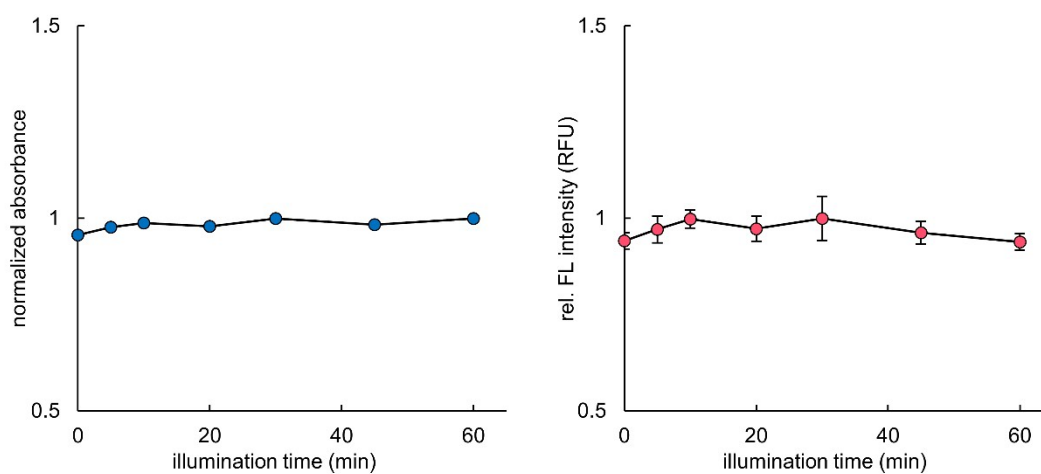
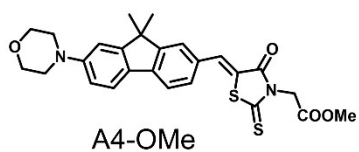
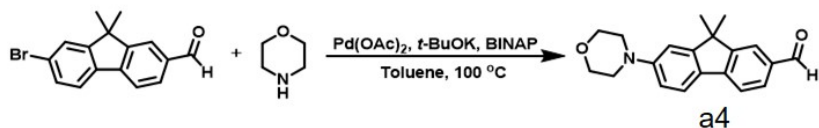
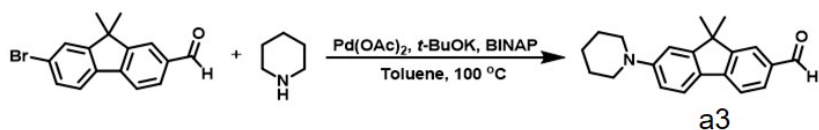
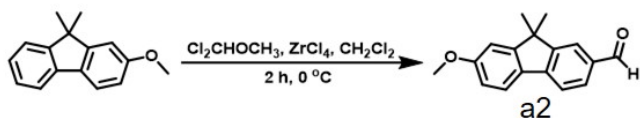
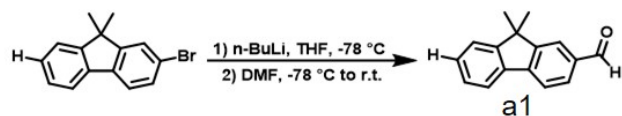


**Figure S13.** A4-OMe remained stable under prolonged exposure to light. 10  $\mu\text{M}$  A4-OMe was illuminated under white light ( $25 \text{ mW}\cdot\text{cm}^{-2}$ ). Samples were taken using 100  $\mu\text{L}$  of the mixed solution at indicated intervals to measure absorbance and fluorescence. Left: absorbance, right: fluorescence. Error bars: standard error ( $n = 3$ ).

### 3. Synthetic Procedures



The aldehyde **a1-a4** were synthesized with reference to the literature.<sup>[22], [23]</sup>

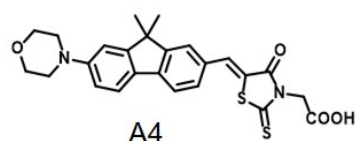
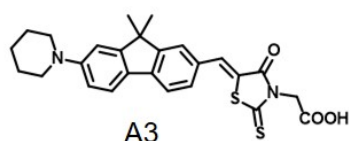
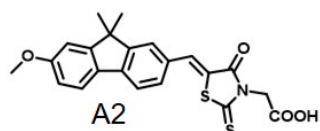
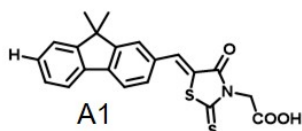
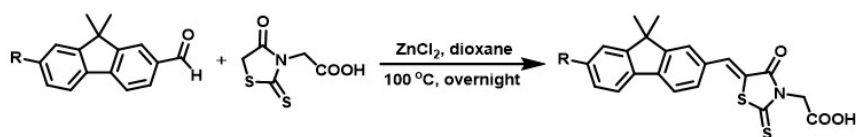
**9,9-dimethyl-9H-fluorene-2-carbaldehyde (a1)**: Light yellow oily liquid (1.53 g, 25.3%). <sup>1</sup>H-NMR (700 MHz, DMSO-*d*<sub>6</sub>):  $\delta$  10.04 (s, 1H), 8.09 (s, 1H), 8.06 (d,  $J = 7.7$  Hz, 1H), 7.96 (m, 1H), 7.93 (m, 1H), 7.62 (m, 1H), 7.41 (m, 2H), 1.48 (s, 6H) ppm. HRMS (*m/z*) Anal. Calc'd for C<sub>16</sub>H<sub>14</sub>O (M+Na)<sup>+</sup>: 245.0937, Found (M+Na)<sup>+</sup>: 245.0938.

**7-methoxy-9,9-dimethyl-9H-fluorene-2-carbaldehyde (a2)**: White powder (0.60 g, 79.0%). <sup>1</sup>H-NMR (700 MHz, DMSO-*d*<sub>6</sub>):  $\delta$  10.40 (s, 1H), 8.11 (s, 1H), 7.84 (d,  $J = 6.9$  Hz, 1H), 7.53 (d,  $J = 7.3$  Hz, 1H), 7.50 (s, 1H), 7.32 (m, 1H), 7.30 (m, 1H), 4.01 (s, 3H), 1.48 (s, 6H) ppm. HRMS (*m/z*) Anal. Calc'd for C<sub>17</sub>H<sub>16</sub>O<sub>2</sub> (M+Na)<sup>+</sup>: 275.1043, Found (M+Na)<sup>+</sup>: 245.1058.

**9,9-dimethyl-7-(piperidin-1-yl)-9H-fluorene-2-carbaldehyde (a3)**: Yellow solid (0.45 g, 48.4%). <sup>1</sup>H-NMR (400 MHz, CDCl<sub>3</sub>):  $\delta$  10.00 (s, 1H), 7.90 (s, 1H), 7.80 (d,  $J = 7.8$  Hz, 1H), 7.69 (d,  $J = 7.9$  Hz, 1H), 7.64 (d,  $J = 8.5$  Hz, 1H), 6.99 (d,  $J = 2.2$  Hz, 1H), 6.94 (m, 1H), 3.29 (t,  $J = 5.4$  Hz, 4H), 1.75 (m, 4H), 1.63 (m, 2H), 1.49 (s, 6H) ppm. HRMS (*m/z*) Anal. Calc'd for C<sub>21</sub>H<sub>23</sub>NO (M+Na)<sup>+</sup>: 328.1672, Found (M+Na)<sup>+</sup>: 328.1654.

**9,9-dimethyl-7-(morpholino)-9H-fluorene-2-carbaldehyde (a4)**: Yellow solid (0.41 g, 33.5%). <sup>1</sup>H-NMR (400 MHz, CDCl<sub>3</sub>):  $\delta$  10.01 (s, 1H), 7.91 (s, 1H), 7.81 (d,  $J = 9.3$  Hz, 1H), 7.72 (d,  $J = 7.8$  Hz, 1H), 7.68 (d,  $J = 8.4$  Hz, 1H), 6.98 (d,  $J = 2.3$  Hz, 1H), 6.93 (m, 1H), 3.90 (t,  $J = 4.8$  Hz, 4H), 3.28 (t,  $J = 4.9$  Hz, 4H), 1.50 (s, 6H) ppm. HRMS (*m/z*) Anal. Calc'd for C<sub>20</sub>H<sub>23</sub>NO<sub>2</sub> (M+H)<sup>+</sup>: 308.1645, Found (M+H)<sup>+</sup>: 308.1633.





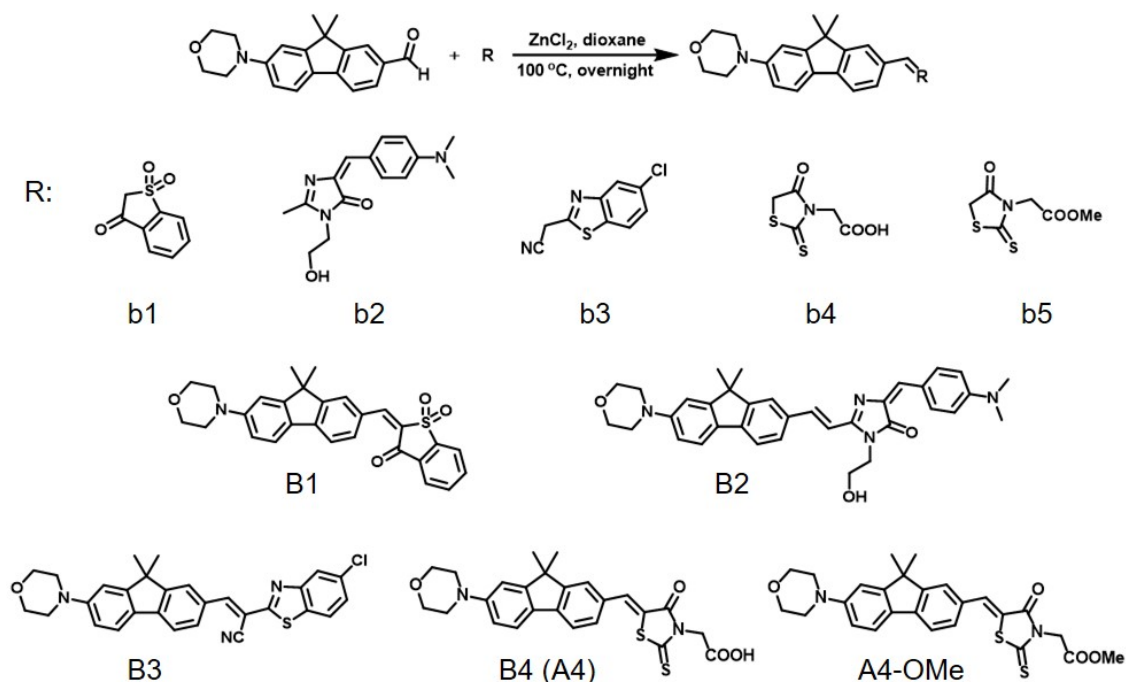
**General Procedures:** Aldehyde **a1-a4** (1.00 equiv.) and rhodanine-3-acetic acid (2.00 equiv.) were combined in dioxane (3 mL/mmol) under argon protection.  $\text{ZnCl}_2$  (1 M in THF, 1.00 equiv.) was added to the reaction and refluxed overnight. After reaction finished, the reaction mixture was diluted with DCM then washed with brine, dried over  $\text{Na}_2\text{SO}_4$ . Organic solvent was removed and crude compound was purified by flash chromatography to yield product **A1-A4**.

**2-(5-((9,9-dimethyl-9H-fluoren-2-yl)methylene)-4-oxo-2-thioxothiazolidin-3-yl)acetic acid (A1):** Yellow solid (0.30 g, 75.1%).  $^1\text{H-NMR}$  (700 MHz,  $\text{DMSO-}d_6$ ):  $\delta$  8.03 (d,  $J = 7.9$  Hz, 1H), 7.97 (s, 1H), 7.94 (m, 1H), 7.84 (s, 1H), 7.67 (dd,  $J = 8.1, 1.7$  Hz, 1H), 7.62 (m, 1H), 7.41 (m, 2H), 4.77 (s, 2H), 1.49 (s, 6H) ppm.  $^{13}\text{C-NMR}$  (176 MHz,  $\text{DMSO-}d_6$ ):  $\delta$  193.2, 167.3, 166.4, 154.4, 154.3, 141.8, 137.3, 134.5, 131.9, 130.4, 128.8, 127.4, 125.3, 123.0, 121.3, 121.2, 120.7, 46.7, 45.1, 26.6 ppm. HRMS ( $m/z$ ) Anal. Calc'd for  $\text{C}_{21}\text{H}_{17}\text{NO}_3\text{S}_2$  ( $\text{M}+\text{H}^+$ ): 396.0723, Found ( $\text{M}+\text{H}^+$ ): 396.0723.

**2-(5-((7-methoxy-9,9-dimethyl-9H-fluoren-2-yl)methylene)-4-oxo-2-thioxothiazolidin-3-yl)acetic acid (A2):** Yellow solid (0.39 g, 91.7%).  $^1\text{H-NMR}$  (700 MHz,  $\text{DMSO-}d_6$ ):  $\delta$  8.05 (s, 1H), 7.86 (m, 2H), 7.54 (d,  $J = 7.4$  Hz, 1H), 7.47 (s, 1H), 7.35 (t,  $J = 6.8$  Hz, 1H), 7.31 (m, 1H), 4.73 (s, 2H), 4.02 (s, 3H), 1.48 (s, 6H) ppm.  $^{13}\text{C-NMR}$  (176 MHz,  $\text{DMSO-}d_6$ ):  $\delta$  193.8, 167.4, 166.6, 159.7, 158.7, 152.8, 137.3, 131.9, 130.0, 127.2, 127.1, 122.7, 121.3, 121.3, 120.4, 119.9, 107.2, 56.2, 47.3, 45.2, 26.6 ppm. HRMS ( $m/z$ ) Anal. Calc'd for  $\text{C}_{22}\text{H}_{19}\text{NO}_4\text{S}_2$  ( $\text{M}+\text{H}^+$ ): 426.0828, Found ( $\text{M}+\text{H}^+$ ): 426.0831.

**2-(5-((9,9-dimethyl-7-(piperidin-1-yl)-9H-fluoren-2-yl)methylene)-4-oxo-2-thioxothiazolidin-3-yl)acetic acid (A3):** Red solid (0.33 g, 67.4%).  $^1\text{H-NMR}$  (700 MHz,  $\text{DMSO-}d_6$ ):  $\delta$  7.92 (s, 1H), 7.82 (d,  $J = 7.9$  Hz, 1H), 7.71 (m, 2H), 7.59 (dd,  $J = 8.0, 1.7$  Hz, 1H), 7.15 (d,  $J = 2.2$  Hz, 1H), 6.94 (dd,  $J = 8.6, 2.3$  Hz, 1H), 4.75 (s, 2H), 3.28 (t,  $J = 5.3$  Hz, 4H), 1.63 (m, 4H), 1.57 (m, 2H), 1.45 (s, 6H) ppm.  $^{13}\text{C-NMR}$  (176 MHz,  $\text{DMSO-}d_6$ ):  $\delta$  193.0, 167.4, 166.4, 156.2, 153.9, 152.6, 142.9, 135.0, 130.8, 129.8, 127.3, 125.0, 122.0, 119.7, 119.0, 114.5, 109.4, 49.2, 46.5, 45.0, 26.8, 25.2, 23.9 ppm. HRMS ( $m/z$ ) Anal. Calc'd for  $\text{C}_{26}\text{H}_{26}\text{N}_2\text{O}_3\text{S}_2$  (M): 478.1385, Found (M): 478.1386.

**2-((9,9-dimethyl-7-morpholino-9H-fluoren-2-yl)methylene)-4-oxo-2-thioxothiazolidin-3-yl)acetic acid (A4):** Red solid (0.19 g, 80.2%). <sup>1</sup>H-NMR (700 MHz, DMSO-*d*<sub>6</sub>): δ 7.91 (s, 1H), 7.85 (d, *J* = 7.9 Hz, 1H), 7.75 (d, *J* = 8.4 Hz, 1H), 7.72 (s, 1H), 7.59 (dd, *J* = 8.0, 1.7 Hz, 1H), 7.18 (d, *J* = 2.3 Hz, 1H), 6.96 (dd, *J* = 8.5, 2.3 Hz, 1H), 4.70 (s, 2H), 3.76 (t, *J* = 4.8 Hz, 4H), 3.24 (t, *J* = 4.9 Hz, 4H), 1.46 (s, 6H) ppm. <sup>13</sup>C-NMR (176 MHz, DMSO-*d*<sub>6</sub>): δ 193.1, 166.5, 156.1, 153.9, 152.1, 142.6, 134.7, 130.7, 130.1, 128.2, 125.0, 122.0, 119.9, 119.4, 114.0, 109.1, 66.1, 48.2, 46.5, 26.8 ppm. HRMS (*m/z*) Anal. Calc'd for C<sub>25</sub>H<sub>24</sub>N<sub>2</sub>O<sub>4</sub>S<sub>2</sub> (M+Na)<sup>+</sup>: 503.107, Found (M+Na)<sup>+</sup>: 503.1085.



**General Procedures:** Aldehyde **a4** (1.00 equiv.) and electron-withdrawing group **b1-b5** (2.00 equiv.) were combined in dioxane (3 mL/mmol) under argon protection. ZnCl<sub>2</sub> (1 M in THF, 1.00 equiv.) was added to the reaction and refluxed overnight. After reaction finished, the reaction mixture was diluted with DCM then washed with brine, dried over Na<sub>2</sub>SO<sub>4</sub>. Organic solvent was removed and crude compound was purified by flash chromatography to yield product **B1-B4** and **A4-OMe**.

**2-((9,9-dimethyl-7-morpholino-9H-fluoren-2-yl)methylene)benzo[*b*]thiophen-3(2H)-one 1,1-dioxide (B1):** Dark red solid (0.18 g, 77.6%). <sup>1</sup>H-NMR (700 MHz, DMSO-*d*<sub>6</sub>): δ 8.38 (d, *J* = 1.7 Hz, 1H), 8.29 (d, *J* = 7.7 Hz, 1H), 8.21 (s, 1H), 8.17 (m, 3H), 8.02 (t, *J* = 7.5 Hz, 1H), 7.94 (d, *J* = 8.0 Hz, 1H), 7.83 (d, *J* = 8.5 Hz, 1H), 7.22 (d, *J* = 2.3 Hz, 1H), 7.01 (dd, *J* = 8.5, 2.3 Hz, 1H), 3.77 (t, *J* = 4.9 Hz, 4H), 3.29 (t, *J* = 4.9 Hz, 4H), 1.48 (s, 6H) ppm. <sup>13</sup>C-NMR (176 MHz, DMSO-*d*<sub>6</sub>): δ 187.9, 178.2, 156.8, 153.5, 152.6, 145.7, 145.1, 143.4, 137.4, 135.0, 134.2, 131.7, 128.2, 127.7, 127.4, 124.6, 122.8, 121.5, 119.6, 114.1, 108.8, 66.0, 47.9, 46.5, 26.8 ppm. HRMS (*m/z*) Anal. Calc'd for C<sub>28</sub>H<sub>25</sub>NO<sub>4</sub>S (M+H)<sup>+</sup>: 472.1577, Found (M+H)<sup>+</sup>: 472.1584.

**2-((E)-2-(9,9-dimethyl-7-morpholino-9H-fluoren-2-yl)vinyl)-5-((E)-4-**

**(dimethylamino)benzylidene)-3-(2-hydroxyethyl)-3,5-dihydro-4H-imidazol-4-one**

**(B2):** Red solid (56.5 mg, 20.1%). <sup>1</sup>H-NMR (700 MHz, DMSO-*d*6): δ 8.18 (m, 2H), 7.96 – 7.59 (m, 4H), 7.26 – 7.13 (m, 1H), 6.91 (m, 1H), 6.85 – 6.73 (m, 5H), 4.92 (s, 1H), 3.82 – 3.51 (m, 6H), 3.04 (m, 6H), 3.00 (s, 6H), 1.35 (m, 6H) ppm. <sup>13</sup>C-NMR (176 MHz, CDCl<sub>3</sub>): δ 171.6, 157.4, 156.8, 156.0, 153.9, 151.8, 151.7, 151.6, 151.5, 134.5, 129.8, 127.8, 123.7, 123.1, 121.9, 121.3, 119.5, 114.8, 112.0, 112.0, 110.0, 107.4, 67.0, 61.6, 49.7, 47.0, 43.4, 40.2, 27.5 ppm. HRMS (m/z) Anal. Calc'd for C<sub>35</sub>H<sub>38</sub>N<sub>4</sub>O<sub>3</sub> (M+H)<sup>+</sup>: 563.3017, Found (M+H)<sup>+</sup>: 563.3017.

**2-(5-chlorobenzo[d]thiazol-2-yl)-3-(9,9-dimethyl-7-morpholino-9H-fluoren-2-**

**yl)acrylonitrile (B3):** Red solid (0.19 g, 78.8%). <sup>1</sup>H-NMR (700 MHz, DMSO-*d*6): δ 8.43 (s, 1H), 8.24 (m, 2H), 8.16 (d, *J* = 2.0 Hz, 1H), 8.09 (dd, *J* = 8.3, 1.7 Hz, 1H), 7.89 (d, *J* = 8.0 Hz, 1H), 7.78 (d, *J* = 8.4 Hz, 1H), 7.56 (dd, *J* = 8.5, 2.1 Hz, 1H), 7.20 (d, *J* = 2.3 Hz, 1H), 6.98 (dd, *J* = 8.5, 2.3 Hz, 1H), 3.77 (t, *J* = 4.8 Hz, 4H), 3.26 (t, *J* = 4.8 Hz, 4H), 1.47 (s, 6H) ppm. <sup>13</sup>C-NMR (176 MHz, CDCl<sub>3</sub>): δ 165.5, 156.9, 154.6, 154.1, 152.5, 148.1, 144.6, 133.3, 133.0, 131.2, 129.9, 129.8, 126.2, 124.5, 123.2, 122.4, 122.2, 119.7, 117.2, 114.8, 109.5, 102.4, 67.0, 49.3, 47.1, 27.3 ppm. HRMS (m/z) Anal. Calc'd for C<sub>29</sub>H<sub>24</sub>ClN<sub>3</sub>OS (M+H)<sup>+</sup>: 498.1401, Found (M+H)<sup>+</sup>: 498.1429.

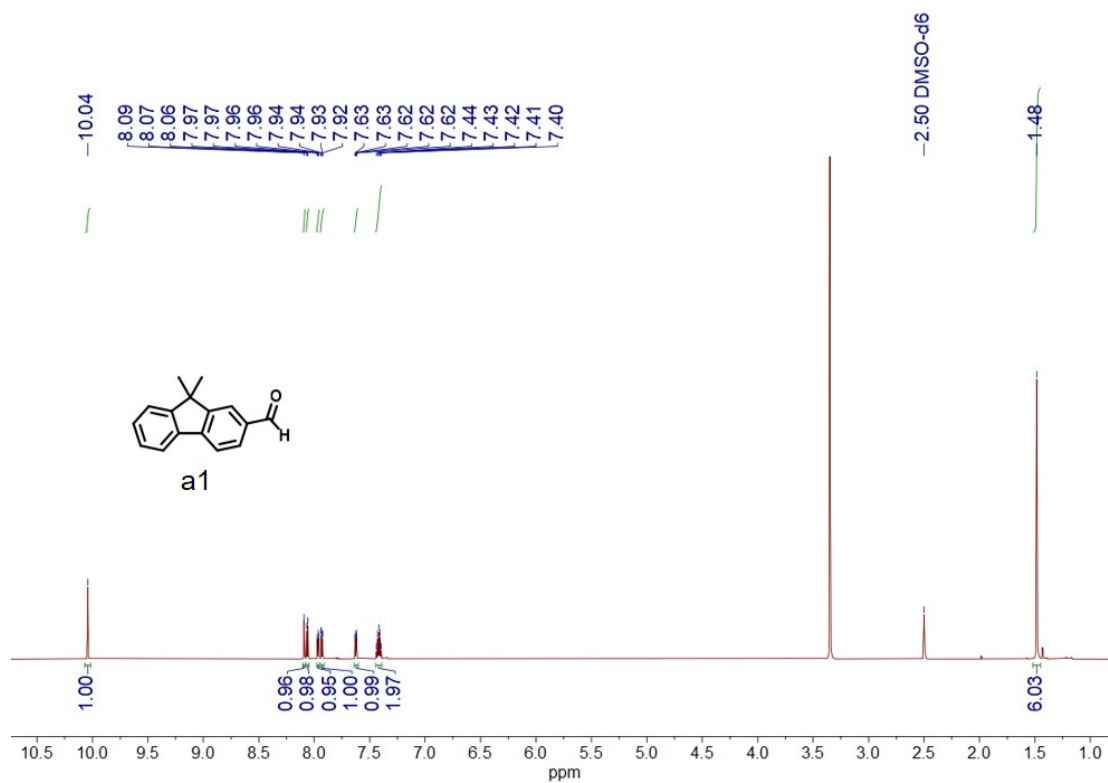
**2-(5-((9,9-dimethyl-7-morpholino-9H-fluoren-2-yl)methylene)-4-oxo-2-**

**thioxothiazolidin-3-yl)acetic acid (B4, i.e. A4):** Red solid (0.19 g, 80.2%). <sup>1</sup>H-NMR (700 MHz, DMSO-*d*6): δ 7.91 (s, 1H), 7.85 (d, *J* = 7.9 Hz, 1H), 7.75 (d, *J* = 8.4 Hz, 1H), 7.72 (s, 1H), 7.59 (dd, *J* = 8.0, 1.7 Hz, 1H), 7.18 (d, *J* = 2.3 Hz, 1H), 6.96 (dd, *J* = 8.5, 2.3 Hz, 1H), 4.70 (s, 2H), 3.76 (t, *J* = 4.8 Hz, 4H), 3.24 (t, *J* = 4.9 Hz, 4H), 1.46 (s, 6H) ppm. <sup>13</sup>C-NMR (176 MHz, DMSO-*d*6): δ 193.1, 166.5, 156.1, 153.9, 152.1, 142.6, 134.7, 130.7, 130.1, 128.2, 125.0, 122.0, 119.9, 119.4, 114.0, 109.1, 66.1, 48.2, 46.5, 26.8 ppm. HRMS (m/z) Anal. Calc'd for C<sub>25</sub>H<sub>24</sub>N<sub>2</sub>O<sub>4</sub>S<sub>2</sub> (M+Na)<sup>+</sup>: 503.107, Found (M+Na)<sup>+</sup>: 503.1085.

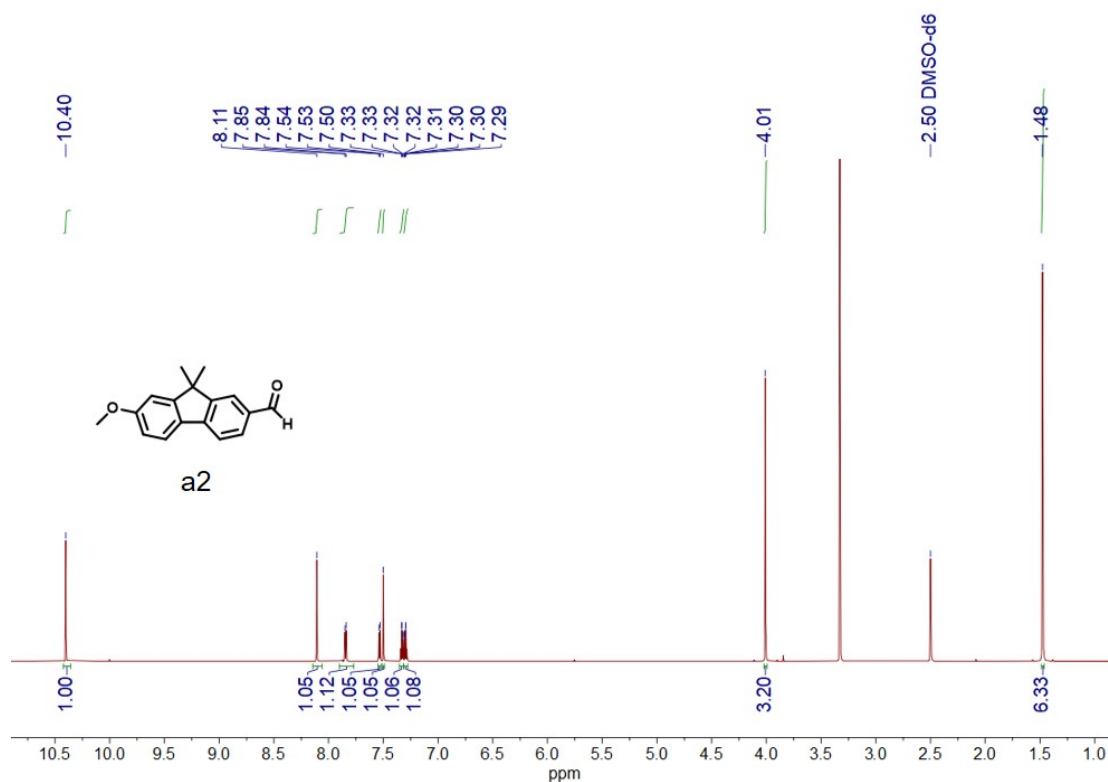
**Methyl-2-(5-((9,9-dimethyl-7-morpholino-9H-fluoren-2-yl)methylene)-4-oxo-2-**

**thioxothiazolidin-3-yl)acetate (A4-OMe):** Red solid (0.10 g, 40.7%). <sup>1</sup>H-NMR (700 MHz, DMSO-*d*6): δ 7.94 (s, 1H), 7.85 (d, *J* = 7.9 Hz, 1H), 7.74 (m, 2H), 7.61 (dd, *J* = 8.0, 1.7 Hz, 1H), 7.19 (d, *J* = 2.3 Hz, 1H), 6.97 (dd, *J* = 8.5, 2.3 Hz, 1H), 4.87 (s, 2H), 3.76 (t, *J* = 4.9 Hz, 4H), 3.71 (s, 3H), 3.25 (t, *J* = 4.9 Hz, 4H), 1.46 (s, 6H) ppm. <sup>13</sup>C-NMR (176 MHz, DMSO-*d*6): δ 193.0, 166.6, 166.3, 156.2, 153.9, 152.2, 142.8, 135.2, 130.8, 130.0, 128.2, 125.0, 122.0, 119.9, 119.1, 114.0, 109.1, 66.1, 52.7, 48.1, 46.5, 44.8, 26.8 ppm. HRMS (m/z) Anal. Calc'd for C<sub>26</sub>H<sub>26</sub>N<sub>2</sub>O<sub>4</sub>S<sub>2</sub> (M+H)<sup>+</sup>: 495.1407, Found (M+H)<sup>+</sup>: 495.1419.

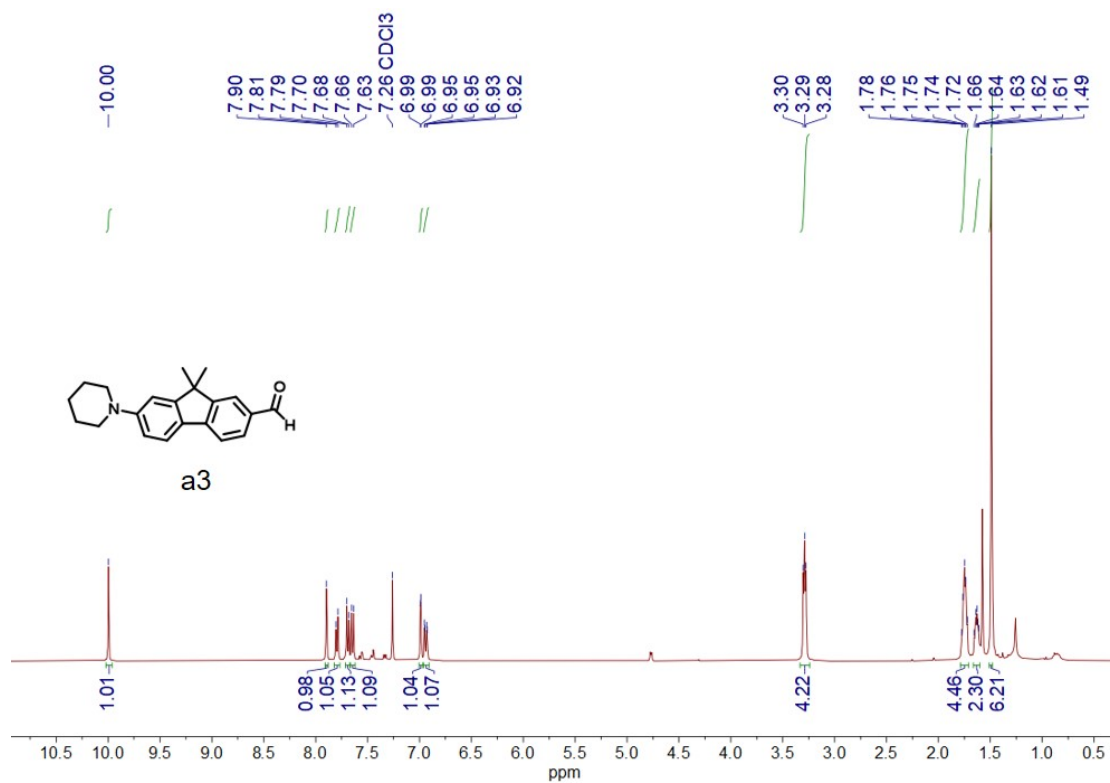
## 4. NMR-Spectra



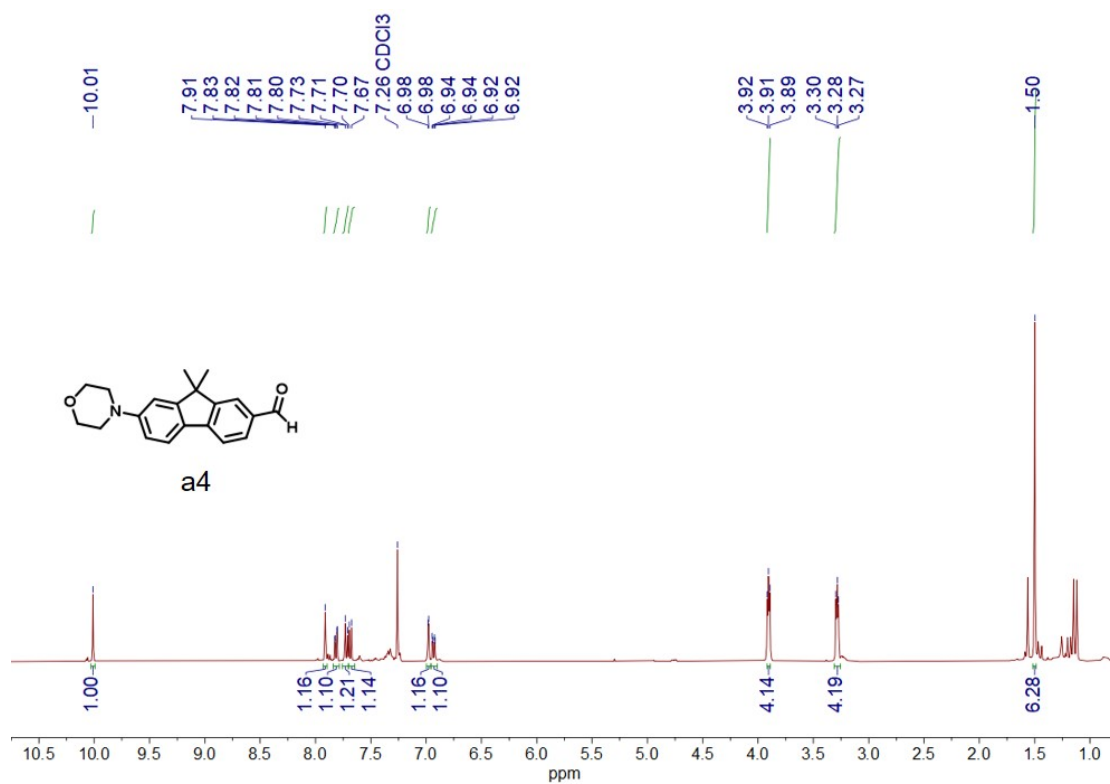
$^1\text{H-NMR}$  spectrum of **a1** ( $\text{DMSO-}d_6$ ).



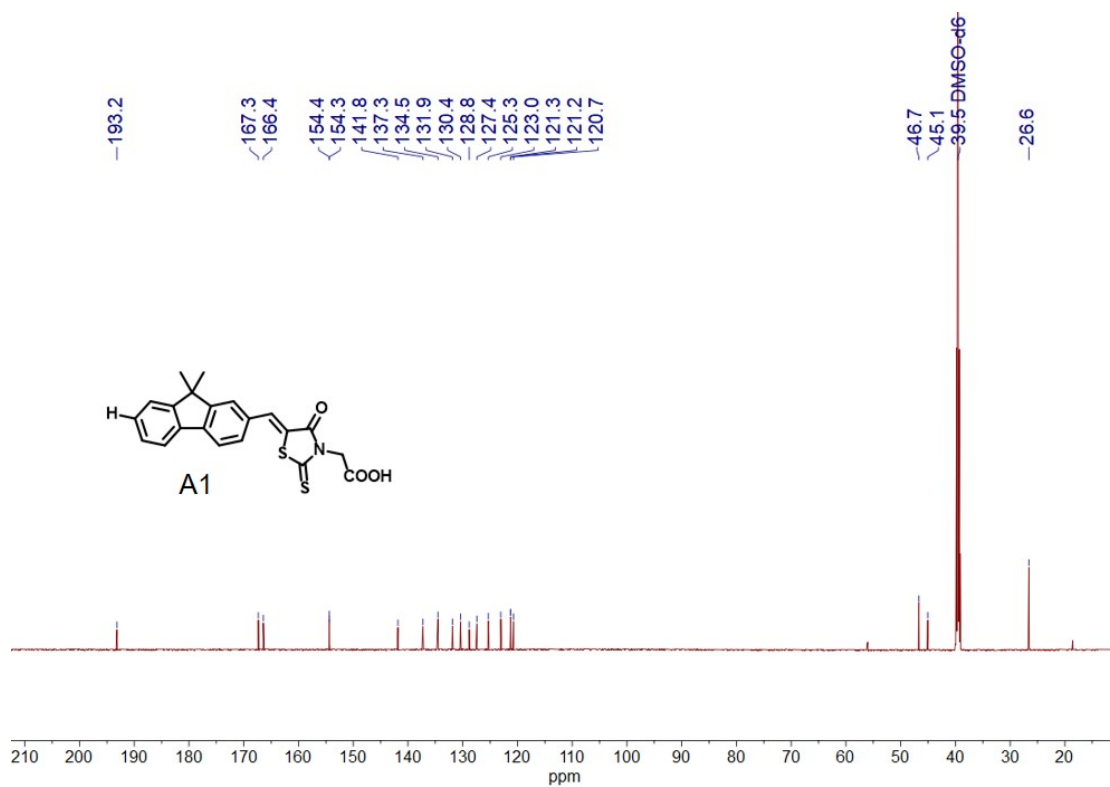
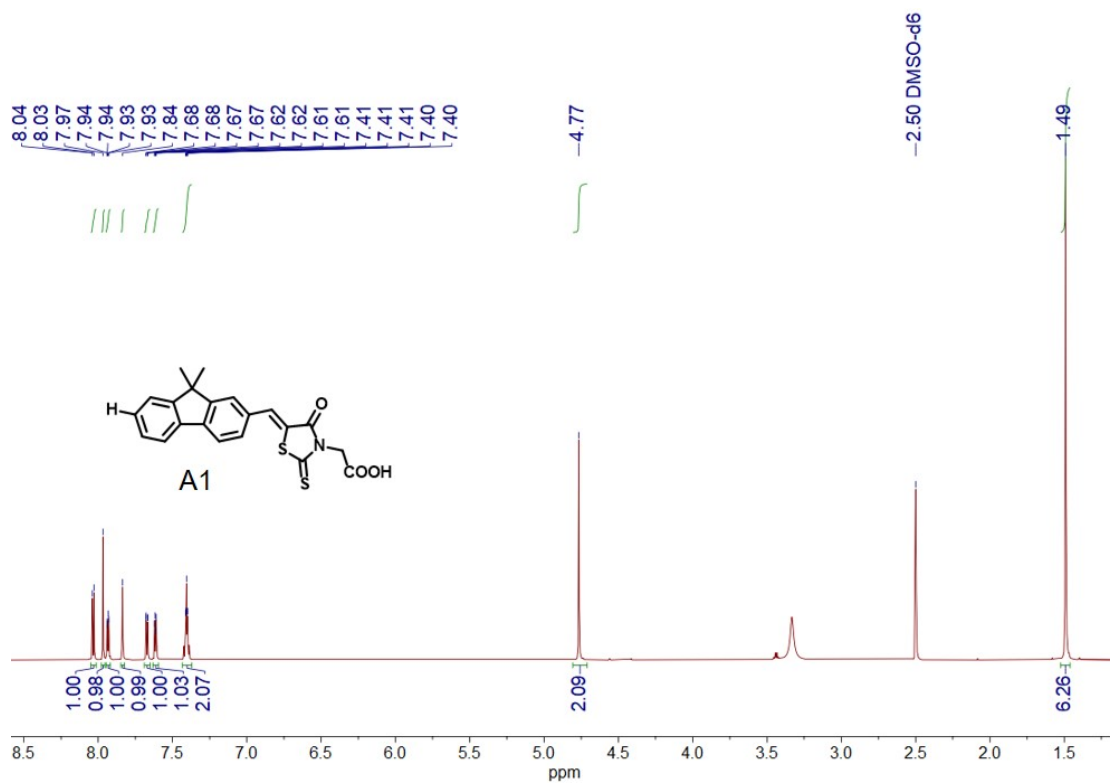
$^1\text{H-NMR}$  spectrum of **a2** ( $\text{DMSO-}d_6$ ).

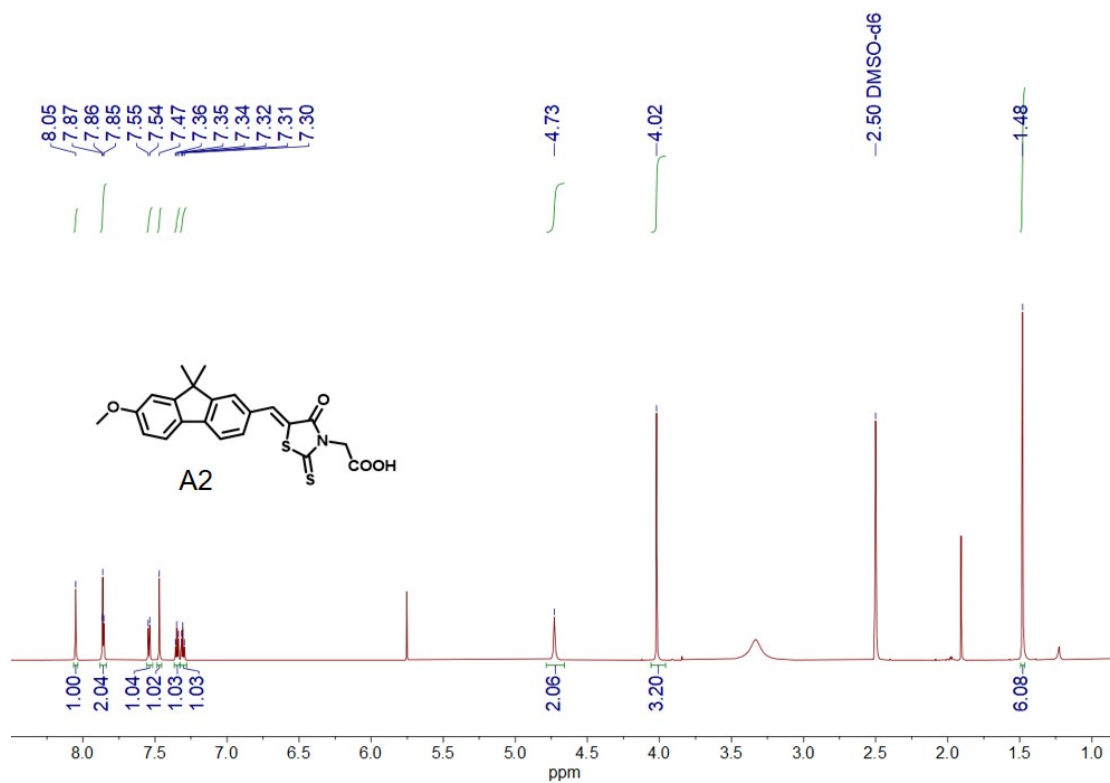


<sup>1</sup>H-NMR spectrum of **a3** (CDCl<sub>3</sub>).

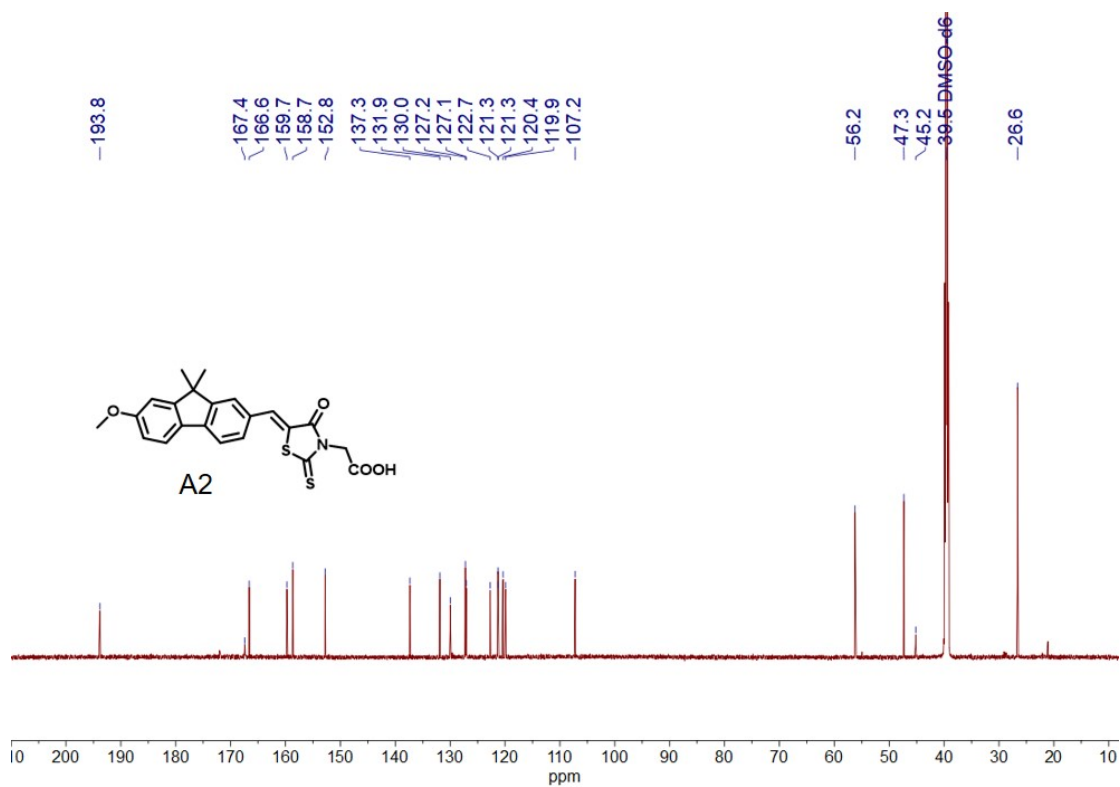


<sup>1</sup>H-NMR spectrum of **a4** (CDCl<sub>3</sub>).

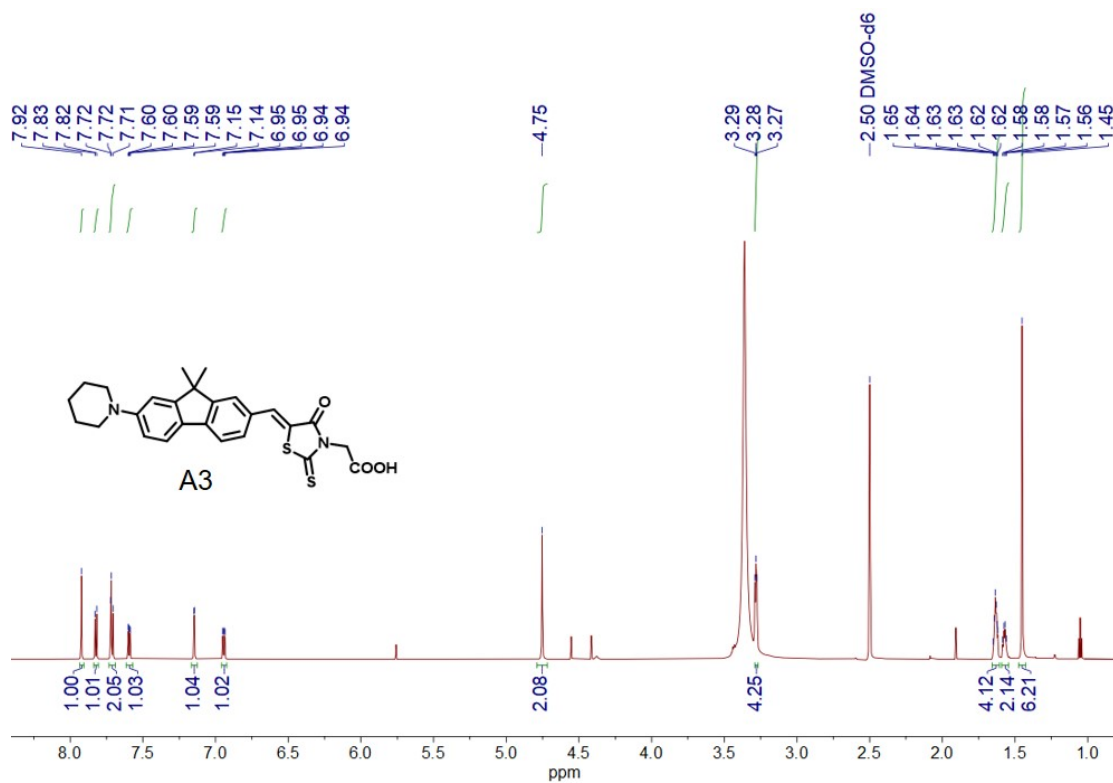




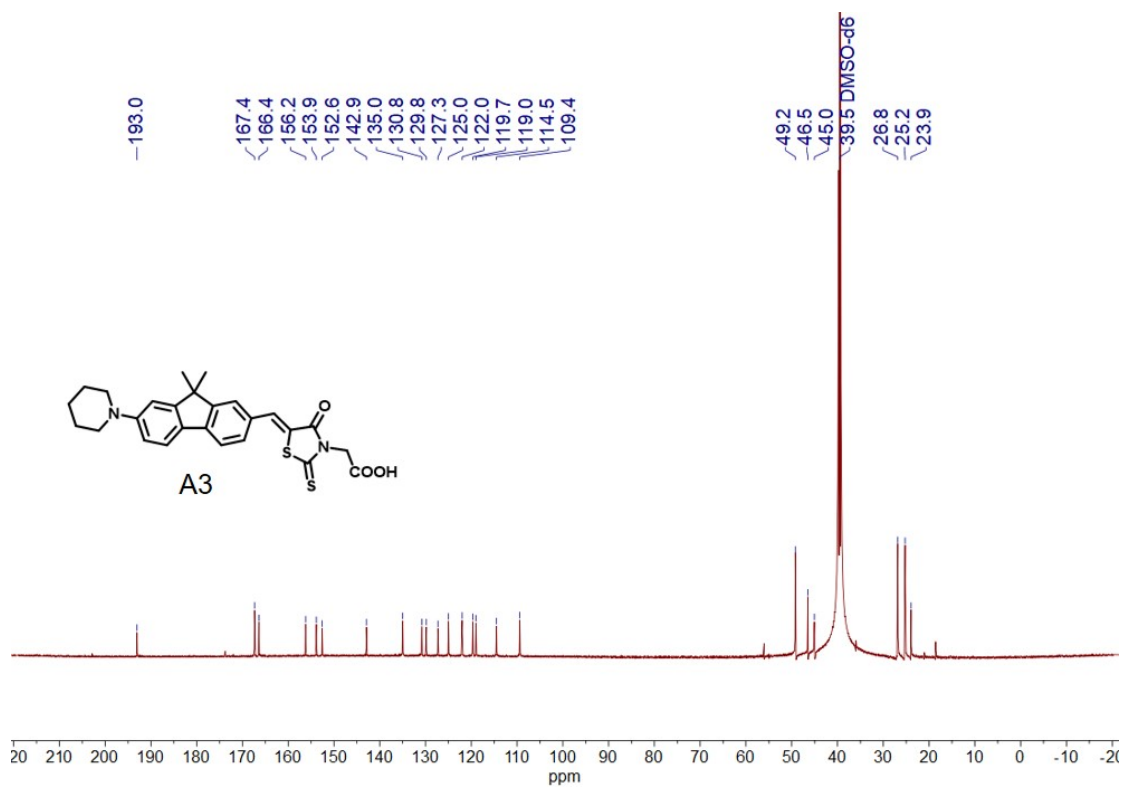
<sup>1</sup>H-NMR spectrum of **A2** (DMSO-d<sub>6</sub>).



<sup>13</sup>C-NMR spectrum of **A2** (DMSO-d<sub>6</sub>).

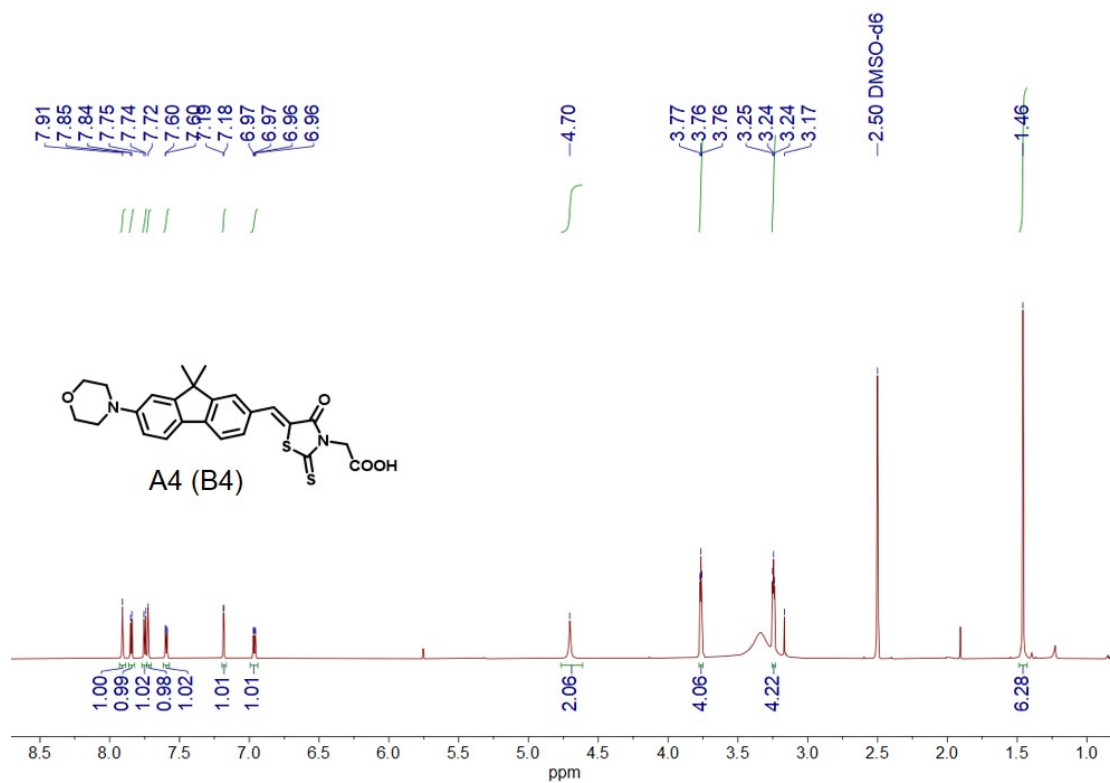


<sup>1</sup>H-NMR spectrum of **A3** (DMSO-*d*<sub>6</sub>).

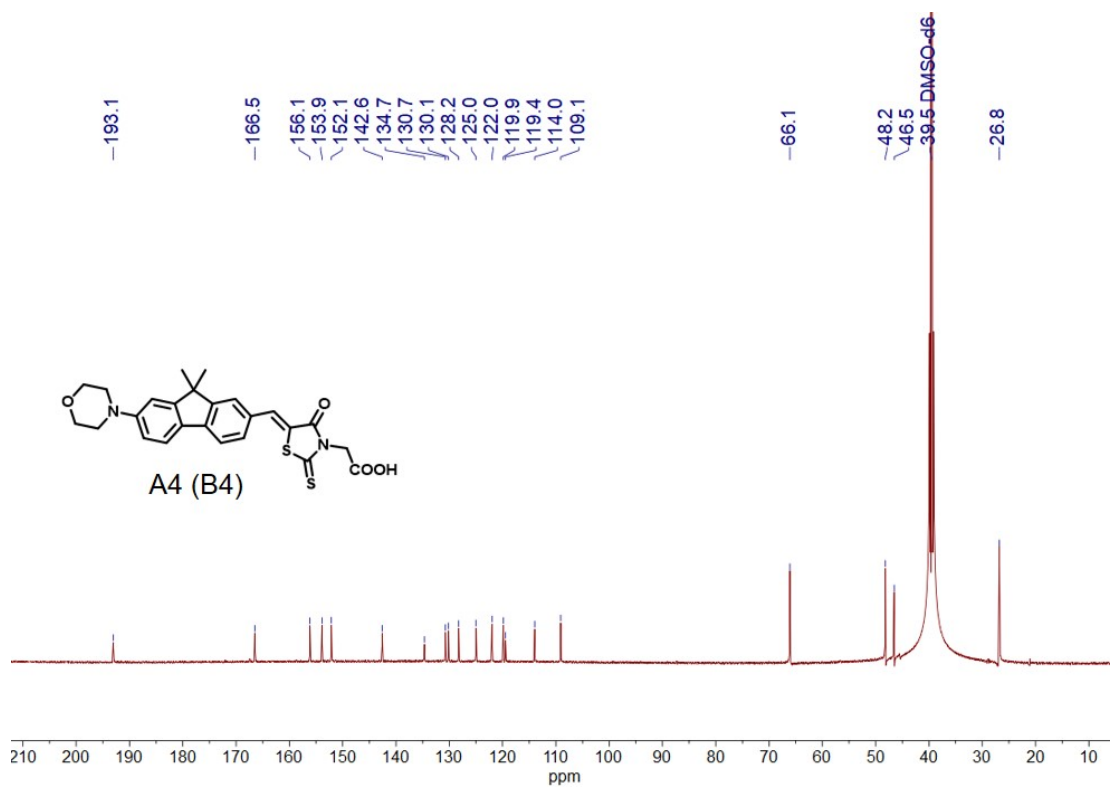


<sup>13</sup>C-NMR spectrum of **A3** (DMSO-*d*<sub>6</sub>).

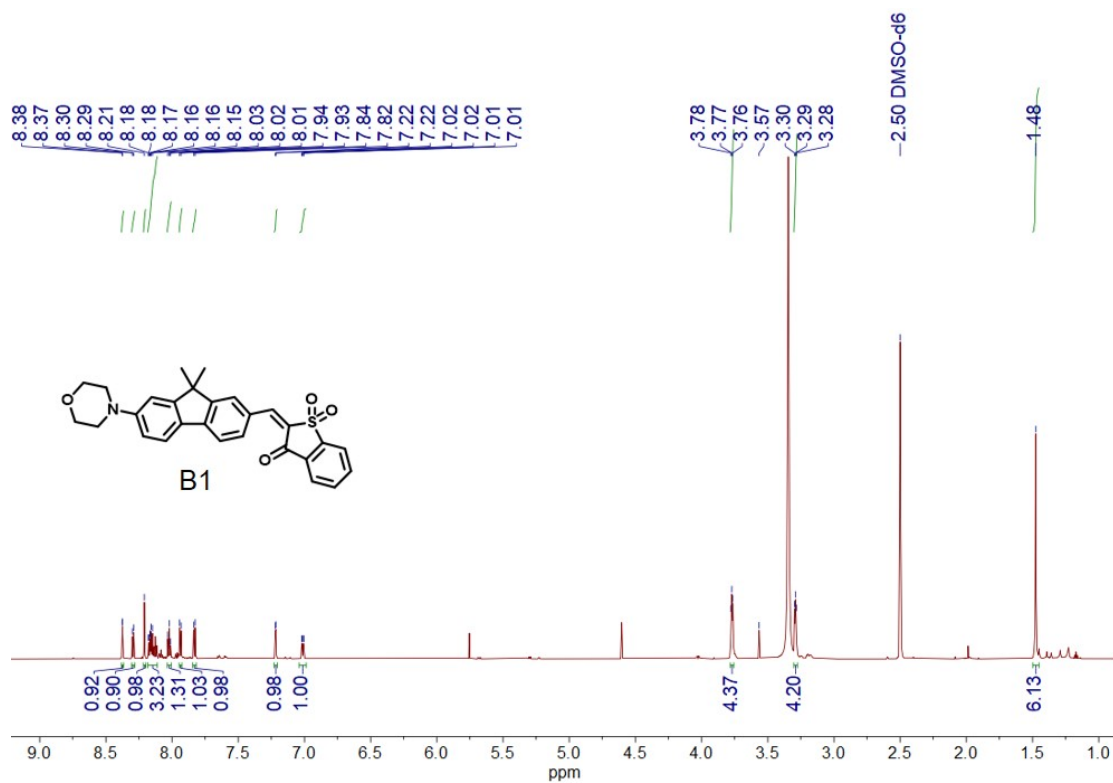




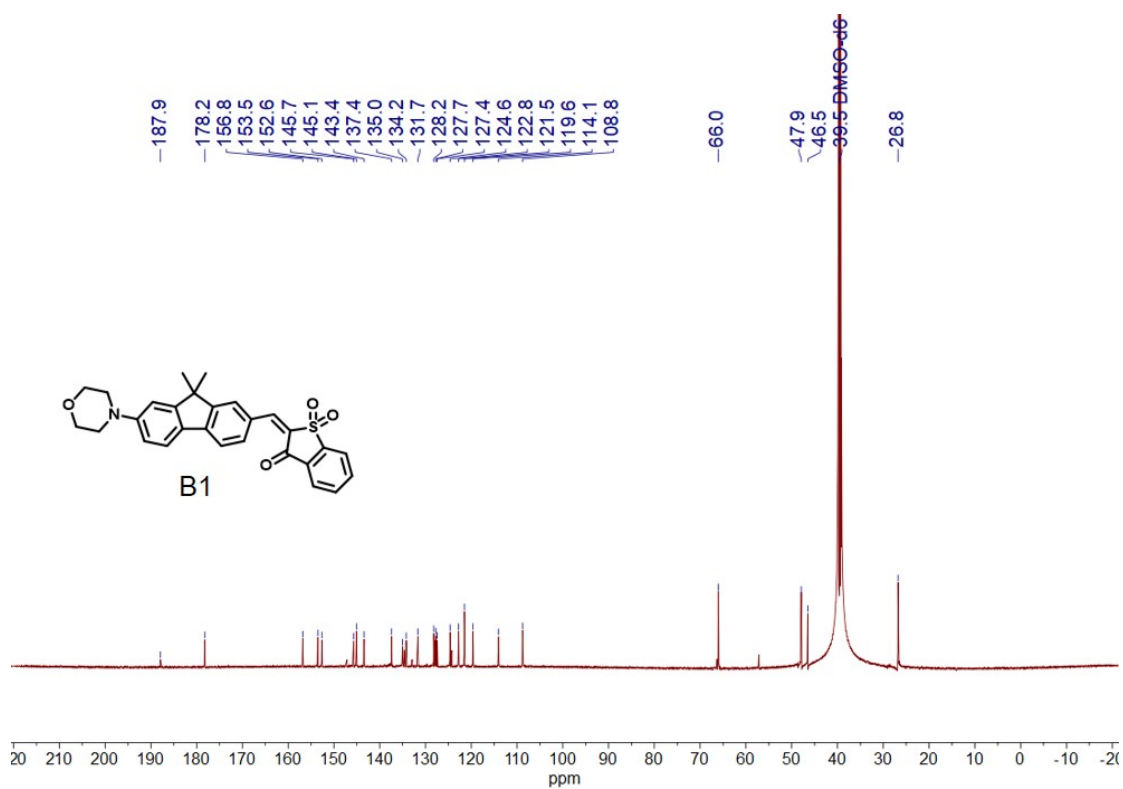
<sup>1</sup>H-NMR spectrum of A4 (B4) (DMSO-d<sub>6</sub>).



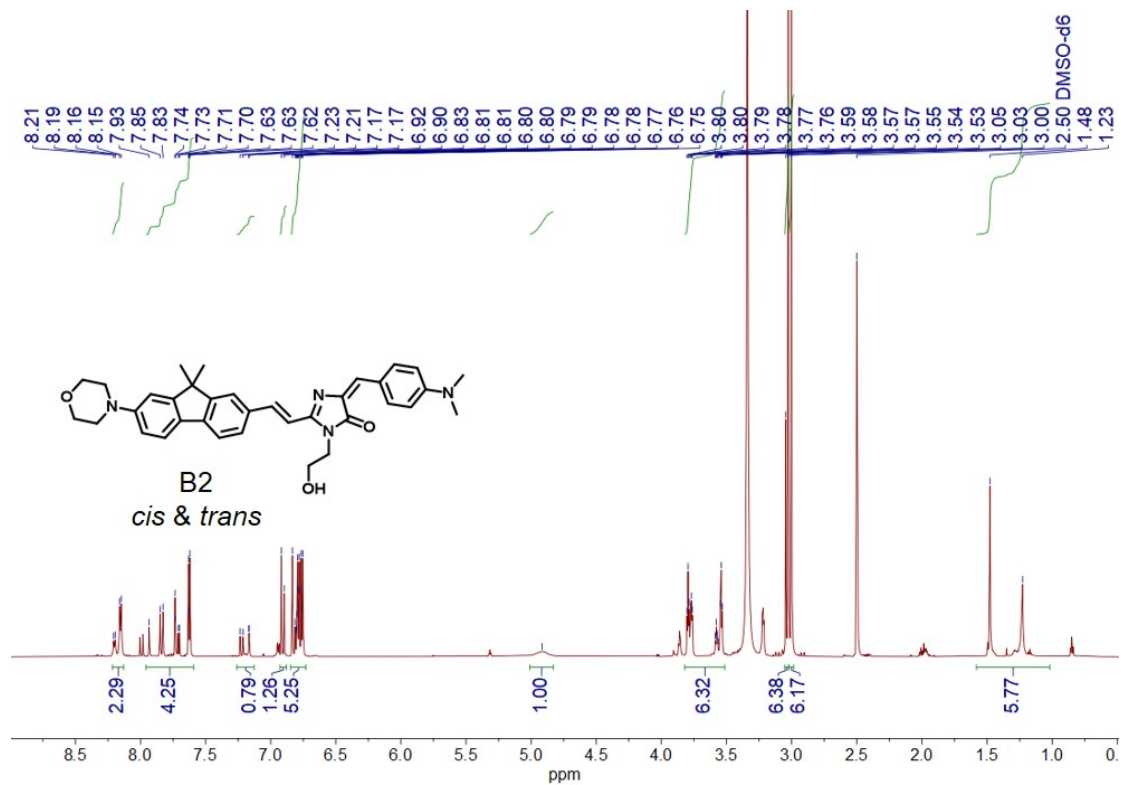
<sup>13</sup>C-NMR spectrum of A4 (B4) (DMSO-d<sub>6</sub>).



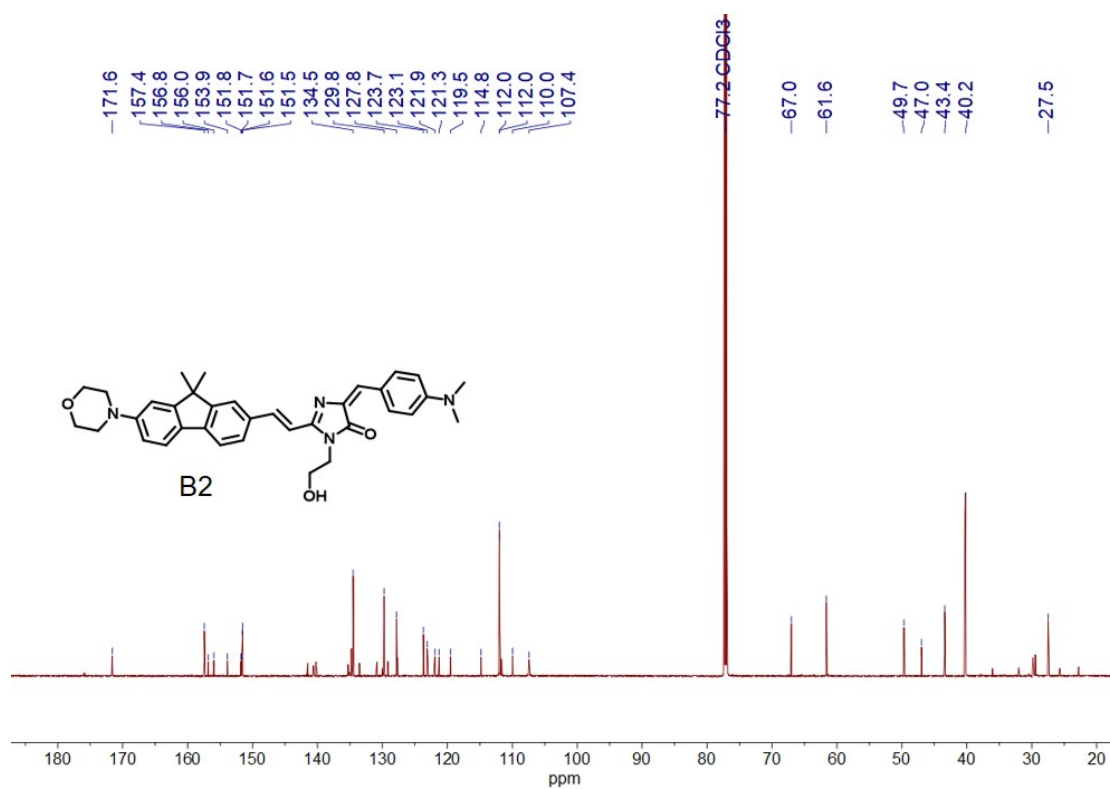
<sup>1</sup>H-NMR spectrum of **B1** (DMSO-*d*<sub>6</sub>).



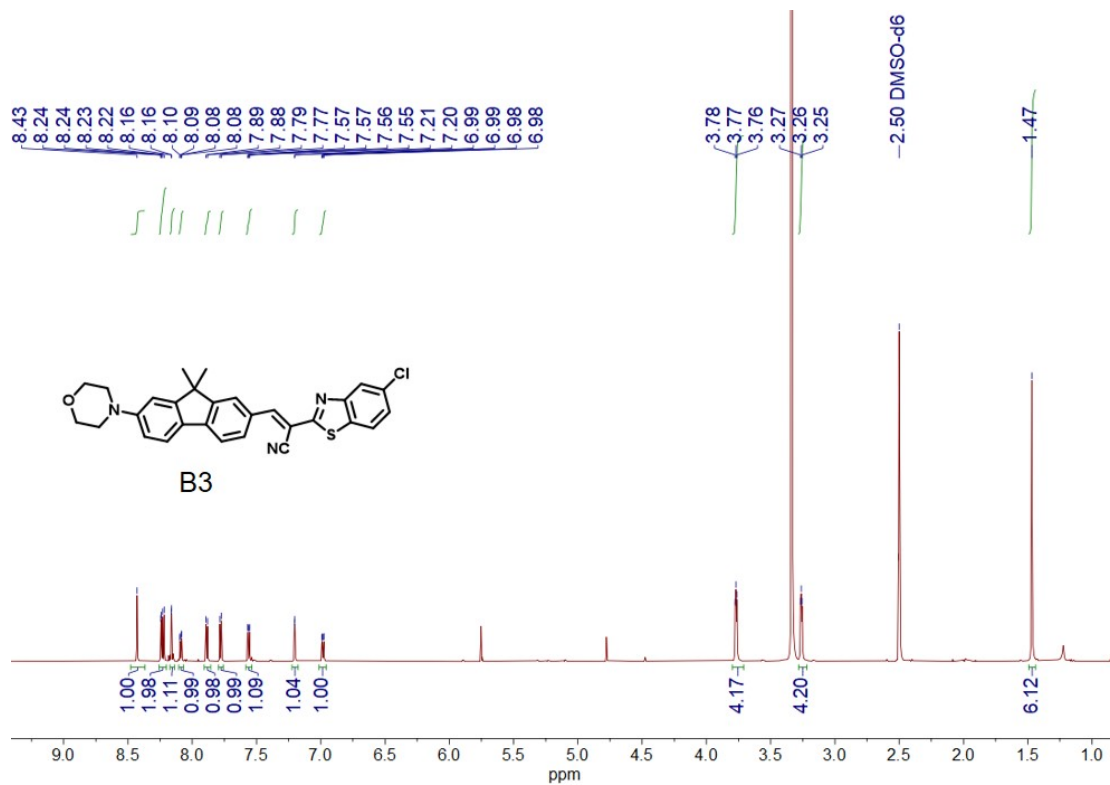
<sup>13</sup>C-NMR spectrum of **B1** (DMSO-*d*<sub>6</sub>).



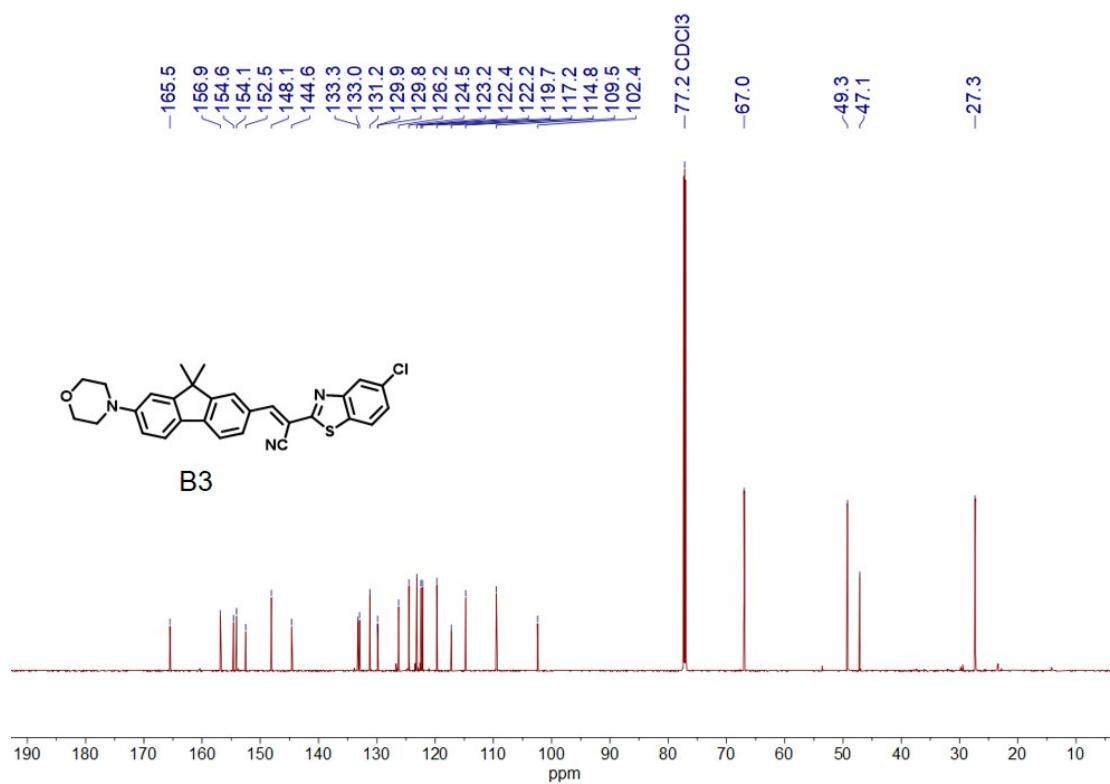
<sup>1</sup>H-NMR spectrum of **B2** (DMSO-*d*<sub>6</sub>).



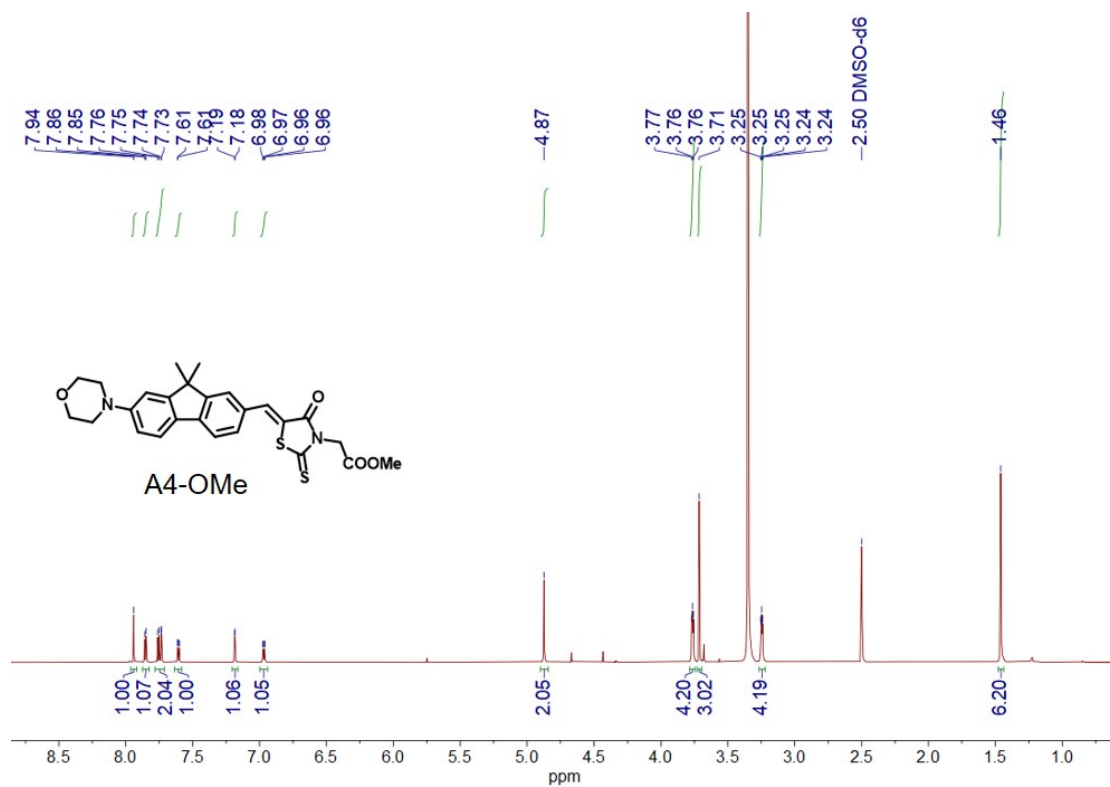
<sup>13</sup>C-NMR spectrum of **B2** (CDCl<sub>3</sub>).



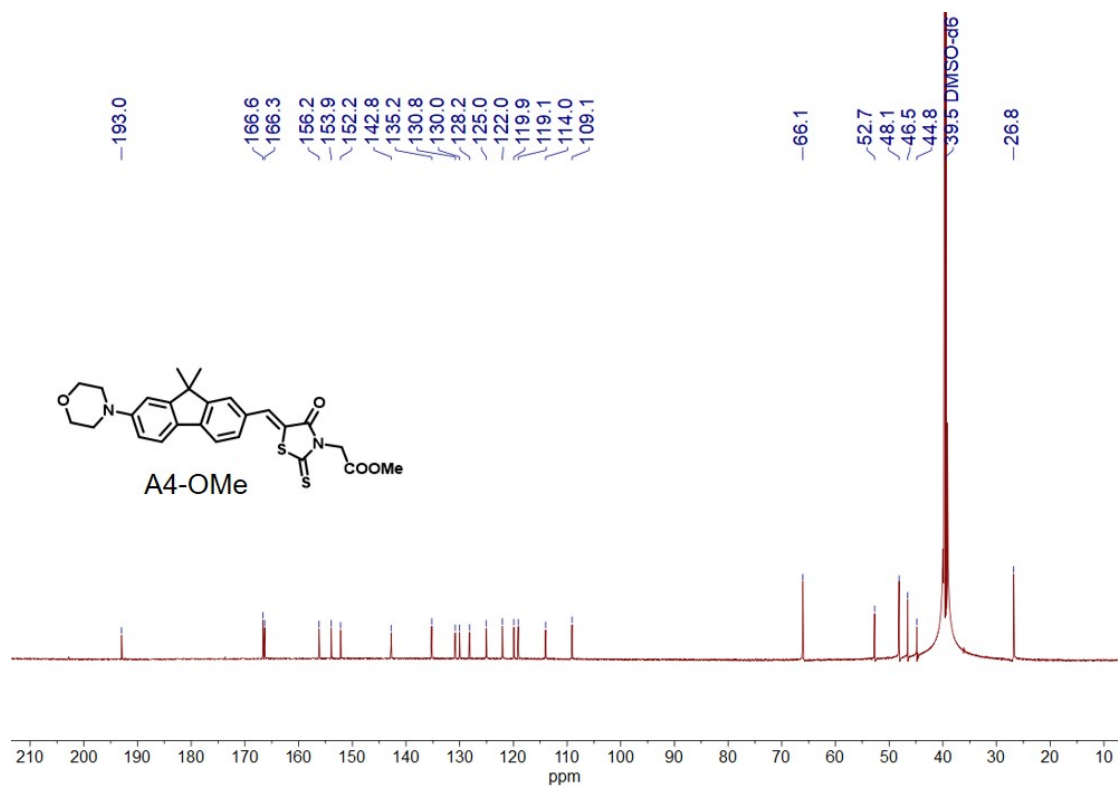
<sup>1</sup>H-NMR spectrum of **B3** (DMSO-*d*<sub>6</sub>).



<sup>13</sup>C-NMR spectrum of **B3** (CDCl<sub>3</sub>).



<sup>1</sup>H-NMR spectrum of **A4-OMe** (DMSO-*d*<sub>6</sub>).



<sup>13</sup>C-NMR spectrum of **A4-OMe** (DMSO-*d*<sub>6</sub>).

## 5. References

- [1] H. Qian, M. E. Cousins, E. H. Horak, A. Wakefield, M. D. Liptak, I. Aprahamian, *Nat. Chem.* **2017**, *9*, 83-87.
- [2] H. J. Yvon, *HORIBA Jobin Yvon Inc, Stanmore, Middlesex, UK* **2012**.
- [3] Baggett, D. W.; Nath, A., *Biochemistry* **2018**, *5*, 6099-6107.
- [4] Yu, Y.; Wu, S.; Zhang, L.; Xu, S.; Dai, C.; Gan, S.; Xie, G.; Feng, G.; Tang, B. Z., *Biomaterials* **2022**, *280*, 121255.
- [5] Feng, H.; Zhao, Q.; Zhang, B.; Hu, H.; Liu, M.; Wu, K.; Li, X.; Zhang, X.; Zhang, L.; Liu, Y., *Angew. Chem. Int. Ed.* **2023**, *62*, e202215215.
- [6] Bu, Y.; Zhu, X.; Wang, H.; Zhang, J.; Wang, L.; Yu, Z.; Tian, Y.; Zhou, H.; Xie, Y., *Anal. Chem.* **2021**, *93*, 12059-12066.
- [7] Guo, J.; Dai, J.; Peng, X.; Wang, Q.; Wang, S.; Lou, X.; Xia, F.; Zhao, Z.; Tang, B. Z., *ACS Nano* **2021**, *15*, 20042-20055.
- [8] Xia, F.; Zuo, X.; Yang, R.; Xiao, Y.; Kang, D.; Vallée-Bélisle, A.; Gong, X.; Heeger, A. J.; Plaxco, K. W., *J. Am. Chem. Soc.* **2010**, *132*, 1252-1254.
- [9] Xia, F.; Zuo, X.; Yang, R.; Xiao, Y.; Kang, D.; Vallée-Bélisle, A.; Gong, X.; Yuen, J. D.; Hsu, B. B. Y.; Heeger, A. J.; Plaxco, K. W., *Proc. Natl. Acad. Sci. U.S.A.* **2010**, *107*, 10837-10841.
- [10] Wang, X.; Nguyen, D. M.; Yanez, C. O.; Rodriguez, L.; Ahn, H.-Y.; Bondar, M. V.; Belfield, K. D., *J. Am. Chem. Soc.* **2010**, *132*, 12237-12239.
- [11] Hosseinzadeh, R.; Mohadjerani, M.; Pooryousef, M., *Luminescence* **2015**, *30*, 549-555.
- [12] Batool, R.; Riaz, N.; Junaid, H. M.; Waseem, M. T.; Khan, Z. A.; Nawazish, S.; Farooq, U.; Yu, C.; Shahzad, S. A., *ACS Omega* **2022**, *7*, 1057-1070.
- [13] Kumar, P.; Kumar, V.; Kaur, N.; Mobin, S. M.; Kaur, P.; Singh, K., *Anal. Chim. Acta* **2022**, *1189*, 339211.
- [14] Junaid, H. M.; Waseem, M. T.; Khan, Z. A.; Munir, F.; Sohail, S.; Farooq, U.; Shahzad, S. A., *ACS Omega* **2022**, *7*, 9730-9742.
- [15] Ding, L.; Zou, Q.; Su, J., *Sens. Actuators B: Chem.* **2012**, *168*, 185-192.
- [16] Verwilt, P.; Kim, H.-R.; Seo, J.; Sohn, N.-W.; Cha, S.-Y.; Kim, Y.; Maeng, S.; Shin, J.-W.; Kwak, J. H.; Kang, C.; Kim, J. S., *J. Am. Chem. Soc.* **2017**, *139*, 13393-13403.
- [17] Elbatrawy, A. A.; Hyeon, S. J.; Yue, N.; Osman, E. E. A.; Choi, S. H.; Lim, S.; Kim, Y. K.; Ryu, H.; Cui, M.; Nam, G., *ACS Sens.* **2021**, *6*, 2281-2289.
- [18] Maruyama, M.; Shimada, H.; Suhara, T.; Shinotoh, H.; Ji, B.; Maeda, J.; Zhang, M.-R.; Trojanowski, John Q.; Lee, Virginia M. Y.; Ono, M.; Masamoto, K.; Takano, H.; Sahara, N.; Iwata, N.; Okamura, N.; Furumoto, S.; Kudo, Y.; Chang, Q.; Saido, Takaomi C.; Takashima, A.; Lewis, J.; Jang, M.-K.; Aoki, I.; Ito, H.; Higuchi, M., *Neuron* **2013**, *79*, 1094-1108.
- [19] Zhao, Y.; Tietz, O.; Kuan, W.-L.; Haji-Dheere, A. K.; Thompson, S.; Vallin, B.; Ronchi, E.; Tóth, G.; Klenerman, D.; Aigbirhio, F. I., *Chem. Sci.* **2020**, *11*, 4773-4778.
- [20] Ono, M.; Hayashi, S.; Matsumura, K.; Kimura, H.; Okamoto, Y.; Ihara, M.; Takahashi, R.; Mori, H.; Saji, H., *ACS Chem. Neurosci.* **2011**, *2*, 269-275.
- [21] Ojida, A.; Sakamoto, T.; Inoue, M.-a.; Fujishima, S.-h.; Lippens, G.; Hamachi, I., *J.*

- Am. Chem. Soc.* **2009**, *131*, 6543-6548.
- [22] Shaya, J.; Fontaine-Vive, F.; Michel, B. Y.; Burger, A., *Chem. Eur. J.*, **2016**, *22*, 10627-10637.
- [23] Xia, Q.; Wan, W.; Jin, W.; Huang, Y.; Sun, R.; Wang, M.; Jing, B.; Peng, C.; Dong, X.; Zhang, R.; Gao, Z.; Liu, Y., *ACS Sens.* **2022**, *7*, 1919-1925.